Storage, mixing and fluxes of water in the critical zone across northern environments inferred by stable isotopes of soil water

Journal:	*Hydrological Processes*
Manuscript ID	HYP-17-0727.R2
Wiley - Manuscript type:	Special issue: Water in the Critical Zone
Date Submitted by the Author:	23-Mar-2018
Complete List of Authors:	Sprenger, Matthias; University of Freiburg, School of Geoscience Tetzlaff, Doerthe; University of Aberdeen, Northern Rivers Institute, School of Geosciences Buttle, James; Trent University, Geography Carey, Sean; McMaster University, Geography & Earth Sciences McNamara, James; Boise State University, Geosciences Laudon, Hjalmar; Swedish University of Agricultural Sciences, Forest Ecology & Management Shatilla, Nadine; McMaster University, Geography & Earth Sciences Soulsby, Chris; University of Aberdeen, School of Geosciences
Keywords:	Isotopes, Soil Hydrology, Fractionation, Northern Environments, Evaporation, Critical Zone

Storage, mixing and fluxes of water in the critical zone across northern environments inferred by stable isotopes of soil water

Matthias Sprenger[1*], Doerthe Tetzlaff[2,3,1], Jim Buttle[4], Sean K. Carey[5], James P. McNamara[6], Hjalmar Laudon[7], Nadine J. Shatilla[5], Chris Soulsby[1]

[1]Northern Rivers Institute, School of Geosciences, University of Aberdeen, Aberdeen, UK (matthias.sprenger@abdn.ac.uk, c.soulsby@abdn.ac.uk)

[2] IGB Leibniz Institute of Freshwater Ecology and Inland Fisheries (d.tetzlaff@igb-berlin.de)

[3] Humboldt University Berlin

[4]School of the Environment, Trent University, Ontario, Canada. (jbuttle@trentu.ca)

[5]School of Geography and Earth Sciences, McMaster University, Hamilton, Ontario, Canada (careysk@mcmaster.ca, shatilnj@mcmaster.ca)

[6]Department of Geosciences, Boise State University, Boise, Idaho, USA (jmcnamar@boisestate.edu)

[7]Department of Forest Ecology and Management, Swedish University of Agricultural Sciences, Umeå, Sweden (hjalmar.laudon@slu.se)

[*]*Correspondence to*: Matthias Sprenger (matthias.sprenger@abdn.ac.uk)

Abstract

Quantifying soil water storage, mixing and release via recharge, transpiration and evaporation is essential for a better understanding of critical zone processes. Here, we integrate stable isotope (^{2}H and ^{18}O of soil water, precipitation, and groundwater) and hydrometric (soil moisture) data from five long-term experimental catchments along a hydroclimatic gradient across northern latitudes: Dry Creek (USA), Bruntland Burn (Scotland), Dorset (Canada), Krycklan (Sweden), and Wolf Creek (Canada). Within each catchment, six to eleven isotope sampling campaigns occurred at two to four sampling locations over at least one year. Analysis for ^{2}H and ^{18}O in the bulk pore water was done for >2500 soil samples either by cryogenic extraction (Dry Creek) or by direct equilibration (other sites). The results showed a similar general pattern that soil water isotope variability reflected the seasonality of the precipitation input signal. However, pronounced differences among sampling locations occurred regarding the isotopic fractionation due to evaporation. We found that antecedent precipitation volumes mainly governed the fractionation signal, temperature and evaporation rates were of secondary importance, and soil moisture played only a minor role in the variability of soil water evaporation fractionation across the hydro-climatic gradient. We further observed that soil waters beneath conifer trees were more fractionated than beneath heather shrubs or red oak trees, indicating higher soil evaporation rates in coniferous forests. Sampling locations closer to streams were more damped and depleted in their stable isotopic composition than hillslope sites, revealing increased subsurface mixing towards the saturated zone and a preferential recharge of winter precipitation. Bulk soil waters generally comprised a high share of waters older than 14 days, which indicates that the water in soil pores are usually not fully replaced by recent infiltration events. The presented stable isotope data of soil water were, thus, a useful tool to track the spatial variability of water fluxes within

and from the critical zone. Such data provide invaluable information to improve the representation of critical zone processes in spatially-distributed hydrological models.

Keywords: Isotopes, Soil Hydrology, Fractionation, Northern Environments, Evaporation, Critical Zone

Running head: Stable isotopes of soil waters in northern environments

1 Introduction

The critical zone is a key determinant of partitioning precipitation into evaporation, transpiration, groundwater recharge, and soil water storage (Brooks et al., 2015). Investigating water storage, mixing and release in the unsaturated soil between the atmosphere and groundwater is therefore crucial for the understanding of processes and interactions within the hydrological cycle (Grant & Dietrich, 2017). The function of the critical zone in providing water for vegetation growth and recharging groundwater resources is increasingly relevant because of observed and projected changes in rain and snow patterns due to climate change (Hartmann et al., 2013) and/or changes in vegetation cover due to land management (Smith et al., 2016). Environments north of 40°N are projected to be most affected by a temperature increase due to climate change (Serreze & Barry, 2011), which can alter snow fall/melt dynamics, soil moisture and vegetation growth in these regions (Holtmeier & Broll, 2005; Xu et al., 2013). As these changes affect the water dynamics of the critical zone in northern latitudes, there is an urgent need for a better understanding of the hydrological processes involved (Tetzlaff et al., 2013).

The upper critical zone, as the interface between soil, vegetation and atmosphere, plays a key role in mediating evapotranspiration and recharge dynamics. Consequently, as vegetation and atmospheric drivers change, the physical understanding of how these drivers affect hydrological processes are pivotal to assess future changes of the critical zone water balance (Brooks et al., 2015; Tetzlaff, Buttle, Carey, van Huijgevoort et al., 2015).

Since predictions of such water balance changes in the critical zone are usually based on hydrological models, we need a sound understanding of the relevant hydrological processes involved to adequately conceptualise them in models in a physically realistic way (Clark et al., 2016). In addition to the hydraulic response of a system, tracers such as stable isotopes of water (^{2}H and ^{18}O) are known to be particularly valuable, since they provide insight into the velocity of water particles and transport (celerity, e.g., measured in soil moisture) processes (McDonnell & Beven, 2014). Accounting for flow velocities enables estimation of water ages (travel times, residence times) in the critical zone, which are of particular interest for contamination transport (e.g., Sprenger, Erhardt, Riedel, & Weiler, 2016) and weathering rates (Maher, 2010). In this regard, the common assumption in tracer-aided hydrological modelling that soils are well-mixed systems is rarely the case in nature (Fenicia et al., 2010; McMillan, 2012), especially when considering the influence of evapotranspiration on the age of runoff (van der Velde et al., 2015).

Previously, field data of stable isotopes of bulk soil water revealed that the water in the unsaturated zone is of varying age (Sprenger, Seeger, Blume, & Weiler, 2016) and that the soil water isotope compositions vary markedly in near-surface soil where vegetation-atmosphere interactions occur (see review by Sprenger, Leistert, Gimbel, & Weiler, 2016). A global analysis by Evaristo, Jasechko, and McDonnell (2015) confirmed that the northern latitudes have not been extensively researched regarding soil water isotope dynamics. Recent work has provided the first insights into isotopic signals into mobile (Geris, Tetzlaff, McDonnell, & Soulsby, 2015; Peralta-Tapia et al., 2016) and bulk soil waters (Geris, Tetzlaff, McDonnell, Anderson et al., 2015; Geris, Tetzlaff, McDonnell, & Soulsby, 2017; Sprenger, Tetzlaff, & Soulsby, 2017a). However, since these studies were limited to single catchments, comparison of how atmospheric conditions and vegetation properties impact the storage, mixing and fluxes of water in the critical

zone at different sites across the northern latitudes is still missing (Tetzlaff, Buttle, Carey, McGuire et al., 2015). We address therefore the following open questions in our study:

- How do atmospheric conditions across a hydroclimatic gradient affect the dynamics of the stable isotopic composition of soil waters?
- Which role do vegetation, topography and elevation play in storage, mixing and flux of water in the critical zone in northern environments?

Our objective is to bring together stable isotope data from five long-term experimental, higher latitude catchments spanning a hydroclimatic gradient regarding their temperature and wetness. We explain their soil water isotope variability in space and time in relation to the environmental conditions. We further present differences and similarities in soil water mixing, percolation and evaporation based on the isotopic signals in soil waters at sampling locations that differ in their vegetation cover, topographic position and elevation. The comparative study reveals the potential for stable isotopes to serve as a tracer to track water through the critical zone.

2 Methods

2.1 Study sites

The study sites are five long-term experimental catchments spanning a hydroclimatic gradient across the northern latitudes: Dry Creek, Idaho, USA (43° 42' N 116° 10' W), Bruntland Burn in the Scottish Highlands, UK (57°2' N 3°7' W), Dorset in south-central Ontario, Canada (45° 12' N 78° 49' W), Krycklan (sub-catchment C4) in northern Sweden (64° 14' N 19° 46′ E), and Wolf Creek in Yukon Territory, Canada (60° 32' N 135° 18' W) (Figure 1). Within each catchment, we sampled the soil water isotopic composition at two to four locations. The catchments are part of the VeWa project (Vegetation effects on water flow and mixing in high-latitude ecosystems,

https://www.abdn.ac.uk/geosciences/departments/geography-environment/vewa-908.php) and their general hydroclimatic and isotopic characteristics have been compared in detail previously (Tetzlaff, Buttle, Carey, van Huijgevoort et al., 2015). For the current study, we focus on the description of the climate and the differences of the sampling locations regarding their soil, vegetation and topographical features (Table 1).

Climatic conditions range from cold arid climate with dry summers (Bsk, according to the updated Köppen-Geiger climate classification by Kottek, Grieser, Beck, Rudolf, and Rubel (2006)) in Dry Creek, warm temperate fully humid climate with cool summers (Cfc) at Bruntland Burn, to cold fully humid climates with either warm summers (Dfb) in Dorset or cold summers (Dfc) in Krycklan, and a cold climate with dry and warm summers (Dsb) in Wolf Creek. Thus, the catchments cover a wide range in air temperatures and precipitation amount. Annual mean air temperature during the sampling period was highest at Dry Creek at 9.5°C and lowest in Wolf Creek at about 0.7°C. Annual precipitation ranges from 440 mm $year^{-1}$ at Wolf Creek to 1332 mm $year^{-1}$ at Bruntland Burn (Table 1).

The soils at Dry Creek are loam to sandy loam soils that developed on granite (Tesfa, Tarboton, Chandler, & McNamara, 2010). At Bruntland Burn, Dorset, and in the freely draining locations at Krycklan and Wolf Creek, podzols have developed on glacial till. The near-stream sampling locations, S04 at Krycklan and RP at Wolf Creek, have considerably higher organic matter content and are classified at Histosols and Alluvium, respectively (Table 1). Soils at all sampling locations are generally of coarse texture ranging between loamy or silty sands to sand (Table 1).

The vegetation cover at each sampling location is listed in Table 1. The Dry Creek locations have a mixed vegetation cover, and the sampling locations at Bruntland Burn are either covered with Scots pine (*Pinus sylvestris*) (NF and SF) or Erica species (*Calluna vulgaris*) (NH and SH).

At Dorset, vegetation at three sampling locations is dominated by coniferous tree cover (Eastern hemlock (*Tsuga canadensis*), Eastern white cedar (*Thuja occidentalis*), White pine (*Pinus strobus*); He, Ce, Pw, respectively) and at one location (Or) by red oak (*Quercus rubra*). Norway spruce (*Picea abies*) is dominant in low-lying areas and Scots pine (*Pinus sylvestris*) in upslope areas at Krycklan, while birch (*Betulaceae nana*) and willow (*Salix spec.*) are dominant at Wolf Creek.

Sampling locations are usually on hillslopes of low gradient, but both the S04 sampling location in Krycklan and the RP sampling location in Wolf Creek are in the riparian zone with groundwater levels < 30 cm (Table 1). Thus, S04 and RP provided a topographical contrast to the upslope locations in the respective catchments: S22 at Krycklan and PL in Wolf Creek.

While the sampling locations within the Bruntland Burn, Dorset, Krycklan and Wolf Creek catchments are at most few hundred metres from each other, the two locations in Dry Creek, one at the catchment outlet (LG) and one at the tree line (TL) are approximately 5 km away from each other and have an altitude difference of 600 m (Table 1).

Environmental conditions at the sampling locations allowed us to investigate the effects of vegetation cover on the soil water isotopic composition at the Bruntland Burn and Dorset sites. The topographical differences between the sites within the Krycklan and Wolf Creek catchments allowed us to compare hillslope soil waters with soil waters in the riparian zone and the different altitudes of the sampling locations at Dry Creek enabled comparison of elevation effects.

2.2 Available data

Soil sampling for the stable isotope analyses occurred between 6 and 11 times at each location over at least one year (Table 2). Sampling during winter dormancy (leaf-off) took place only on a

few occasions. The maximum sampling depths at the locations varied between -20 cm at Bruntland Burn and -70 cm at Dry Creek and depended mainly on the accessibility of the soil which decreased over depth with increasing rock content. At Bruntland Burn, Krycklan and Dorset soil samples were taken in 5 cm intervals down to 20, 30 or 50 cm depths, respectively. At each depth five (Bruntland Burn and Krycklan) or four (Dorset) replicates within 10 m distance were taken for every sampling campaign. However, due to the high rock content, it was not always possible for four replicates to be taken at depths below 20 cm at the Dorset locations. Sampling depths at Dry Creek were 10, 25, 45, and 70 cm and number of replicates varied between 2 and 4 at each depth and sampling day due to varying rock contents. The sampling depths at Wolf Creek varied between 2 cm for the shallowest and 40 cm for the deepest samples and were therefore grouped into 10 cm intervals and the number of replicates varied between 1 and 3.

The stable isotopic compositions ^{2}H and ^{18}O of soil water was sampled with the direct-equilibration method proposed by Wassenaar, Hendry, Chostner, and Lis (2008) for Bruntland Burn, Dorset, Krycklan, and Wolf Creek. A detailed description of stable isotope analyses as done at the University of Aberdeen for the European samples was presented by Sprenger, Tetzlaff, and Soulsby (2017b) and for the Canadian samples analysed at the University of Saskatchewan was described by Hendry, Schmeling, Wassenaar, Barbour, and Pratt (2015). The general procedure for the direct-equilibration method was as follows: disturbed soil samples were stored in sealed bags and dry air was added to the bag in the laboratory. During 2 or 3 days (University of Aberdeen and Saskatchewan, respectively) of storage at constant temperature, an isotopic equilibration between the soil water and the headspace developed and then the vapour of the saturated headspace was sampled directly via laser spectrometry (TWIA-45-EP LGR). Bags

with standard waters of known isotopic composition ranging the expected soil water isotopic composition were also analysed the same way. These standard waters were used for calibration to derive the isotopic composition of the liquid soil waters from the vapor measurements in reference to the Vienna standard mean ocean water (VSMOW) as proposed by Wassenaar et al. (2008). Water from soil samples taken at Dry Creek were cryogenically extracted at 100°C under vacuum of < 30 millitorr over 40 minutes (McCutcheon, McNamara, Kohn, & Evans, 2016). The accuracy of the direct-equilibration method was ±0.31 ‰ for $\delta^{18}O$ and ±1.13 ‰ for $\delta^{2}H$ (Sprenger et al., 2017a) and ±0.15 ‰ for $\delta^{18}O$ and ±0.69 ‰ for $\delta^{2}H$ for the cryogenic extraction (West, Patrickson, & Ehleringer, 2006). Based on comparisons between the direct-equilibration and cryogenic extraction method on field wetted silty to sandy soils (Orlowski, Pratt, Breuer, & McDonnell, 2017; Sprenger, Herbstritt, & Weiler, 2015), we can assume that the differences regarding the shape of the isotope depth profiles between these two methods are not significant. The soil samples analysed with the direct-equilibration are more enriched in heavy isotopes than the samples analysed with the cryogenic extraction. However, the differences plot along the LMWL in a dual-isotope plot. Both analysis methods are not limited to sampling the mobile water, but generally determine the stable isotopic composition of bulk soil water (Sprenger et al., 2015).

Along with the soil water sampling, precipitation and snow melt from lysimeters were sampled for their isotopic composition at each catchment. Daily precipitation samples were available at Bruntland Burn and Krycklan. Daily to fortnightly data were available at Dorset, Dry Creek, and Wolf Creek. Snow melt was sampled at Dry Creek, Dorset, Krycklan, and Wolf Creek with snow lysimeters. Snowmelt is not relevant at the Bruntland Burn site. Isotopic analyses of precipitation and snow melt were done on a Los Gatos DLT-100 laser isotope analyser for Dorset and Wolf

Creek, a Los Gatos Liquid Water Isotope Analyzer (LWIA) for Bruntland Burn and Dry Creek, and on a Picarro L1102-i and L2130-I for Krycklan. The precision of the liquid water stable isotope analysis is reported to be better than ±0.1 ‰ for $\delta^{18}O$ and ±0.4 ‰ for $\delta^{2}H$. All isotope data are given in delta-notation (Coplen, 2011) in reference to the VSMOW.

We derived the local meteoric water line (LMWL) for each catchment, describing the linear relationship between $\delta^{2}H$ and $\delta^{18}O$ values in precipitation samples as a regression line of slope *a* and the intercept *b*: $\delta^{2}H = a * \delta^{18}O + b$. Water samples plotting along the LMWL in a dual isotope plot represent equilibrium fractionation (at 100% humidity) as described by Majoube (1971). Water samples located below the LMWL are indicative of non-equilibrium (kinetic) fractionation, which occurs during evaporation in open systems at humidity below 100% (Gat & Gonfiantini, 1981). This deviation from the LMWL was defined by Landwehr and Coplen (2006) as the line-conditioned excess (lc-excess) as follows: lc-excess $= \delta^{2}H - a * \delta^{18}O - b$, using slope *a* and intercept *b* of the LMWL.

In addition to the isotope data, standard meteorological data including air temperature (T) and precipitation amount (P) were available at each catchment. Further, potential evapotranspiration (PET) was estimated using the Penman-Monteith equation (Allen, Pereira, Raes, & Smith, 1998). From this, we generated mean values to characterize the hydro-meteorological conditions prior to the soil sampling campaigns: P_2, P_7, P_{14}, and P_{30}: sum of precipitation and snowmelt input over 2, 7, 14 and 30 days prior to soil sampling, respectively, PET_{30}: average potential evapotranspiration 30 days prior to soil sampling, T_{30}: mean air temperature 30 days prior to soil sampling, DD_{30}: number of dry days in 30 days prior to soil sampling. Regarding T_{30}, PET_{30} and DD_{30}, the time span of integration does not affect the analysis, as the 30-day indices correlate

linearly with indices of time spans of 2, 7, or 14 days. As precipitation sums over 2, 7, 14, or 30 days do not necessarily correlate, we tested in our analysis different integration periods.

Daily soil moisture data based on continuous soil moisture measurements at 10 or 15 cm soil depth were available for each soil water sampling location at Bruntland Burn, Dry Creek, Krycklan, and Wolf Creek (Figure S1), representing the soil water storage in the top soil. For Dorset, where only a few manual soil moisture measurements were available, daily soil moisture data were derived from soil physical modelling as shown by Sprenger, Tetzlaff, Buttle, Laudon, Leistert et al. (2018). The volumetric soil moisture (VSM, $cm^3\ cm^{-3}$) data were used to assess the hydrologic state (e.g., wetness) on the days of individual sampling campaigns.

2.3 Statistical analysis

Comparisons between differences in soil water δ^2H and lc-excess in the upper 10 cm and soil below 10 cm were done with the Wilcoxon rank sum test (Hollander & Wolfe, 1973) adjusting p-values according to Holm (1979), as the data sets were not normally distributed according to the Shapiro-Wilk test. We analysed linear relationships between average soil water δ^2H, $\delta^{18}O$, or lc-excess of the sampling sites and weighted average of P δ^2H, P $\delta^{18}O$, or P lc-excess, respectively, using Pearson correlation, as the data sets were normally distributed according to the Shapiro-Wilk test. The same applied to relationships of average P δ^2H and P $\delta^{18}O$ with average air temperature at the catchments. Spearman rank correlation was used for analysis of relationships of soil water δ^2H and lc-excess with P_{30}, T_{30}, VSM, and P_{30} δ^2H or P_{30} lc-excess, respectively, at each site, as normality could not be assumed for all data sets based on the Shapiro-Wilk test.

We used multiple linear regression (MLR) to assess which variables explain the variance of the soil water lc-excess over time (over a year, spring, summer, and autumn) and space (between sampling locations). For the MLR, we derived mean values for each sampling location for lc-excess in the top 30 cm, as the upper 30 cm of soil has been shown to be most affected by evaporation fractionation (Sprenger, Leistert et al., 2016). While the sampling depths were not the same at Dry Creek and Wolf Creek as at the other sites, we still saw at all sites the highest dynamics of lc-excess in the upper soil layer, which allowed inferring evaporation fractionation from such data. Just like the lc-excess values, we calculated average values of the possible predictors P_2, P_7, P_{14}, P_{30}, T_{30}, PET_{30}, DD_{30}, VSM for all sampling campaigns considered, and data taken in spring, summer, and autumn, respectively. We reduced the number of possible predictors to P_7, P_{30}, T_{30}, and VSM as correlation diagrams revealed collinearity of T_{30} with PET_{30} and P_{30} with DD_{30} (Figure S4, S5, S6, S7). Multiple linear regression analysis was then applied (including interaction of the predictors) and non-significant predictors were discarded subsequently to simplify the model. The significance of predictors was tested with ANOVA ($p < 0.05$). The final MLR model only considered significant predictors. All the data used in the MLR were standardized to account for differences in the units and ranges of the predictors (z-scores transformation). We also tested whether using logarithmic or exponential transformation of variables improved the regression fit. The soil water lc-excess data were reciprocally transformed for the MLR conducted on the entire data set and the subset of summer samples to get normal distributions. The autumn data was not normally distributed and also transformation did not result in normal distribution of lc-excess values. The relative importance of the explanatory parameters in the MLR model were derived according to Grömping (2006). To visualize relationships between potentially non-linear and/or statistically non-significant trends,

we added LOWESS (Locally Weighted Scatterplot Smoothing) curves to scatter plots (Cleveland, 1979).

We used Pearson correlation to assess the relationships between soil water δ^2H at different depths and the weighted precipitation δ^2H values integrated over 2, 7, 14 and 30 days, respectively, as the hypothesis of the data being normally distributed could not be rejected (Shapiro-Wilk test). The average weighted precipitation input over 30 days prior to the sampling showed highest correlation, which is why we also provide the slope of the regression for soil water δ^2H at different depths and P_{30} input δ^2H compositions.

3 Results

3.1 Stable isotope dynamics in soil waters across a hydroclimatic gradient

3.1.1 Variability at each sampling location

Soil water isotopic composition (δ^2H and $\delta^{18}O$) across the five catchments reflected the isotopic composition of the local precipitation input (P) (Figure 2, Table 2). The average soil water δ^2H and $\delta^{18}O$ values in the upper 30 cm at each sampling location correlated significantly with the corresponding weighted average of precipitation ($r = 0.94$ and $r = 0.92$, respectively, and both $p < 0.001$). The weighted average of P δ^2H was related to the annual average air temperature across the hydroclimatic gradient between Bruntland Burn, Dorset, Krycklan and Wolf Creek ($r = 0.98$, $p = 0.02$). The precipitation isotope data from Dry Creek were excluded for this correlation, as precipitation mainly falls during winter leading to depleted average precipitation/snow melt isotope compositions similar to Krycklan, despite the air temperature being on average ~5 °C warmer in Dry Creek (Table 1).

The seasonality of P δ^2H and P $\delta^{18}O$ was imprinted in the sampled soil water isotope depth profiles (Figure S2). The soil water δ^2H profiles showed more depleted values between late autumn and early spring compared to sampling campaigns during summer and early fall that were generally more enriched. The soil water δ^2H and $\delta^{18}O$ of the upper 30 cm at the individual sampling locations showed limited relationships with the potential explanatory variables: δ^2H P_{30}, P_{30}, T_{30}, VSM (Table S1). Soil water lc-excess dynamics at the individual sampling locations also could not be related to lc-excess P_{30}, P_{30}, T_{30}, or VSM (Table S1).

At all sites, the top 10 cm were significantly more enriched in both δ^2H and $\delta^{18}O$ compared to soil water below 10 cm (Figure 2b). Soil waters in the top 10 cm often plotted below the LMWL and the lc-excess showed that the evaporation signal was significantly more pronounced in the top 10 cm than below 10 cm at Bruntland Burn, Dorset and Dry Creek during the growing season when evaporative demand was highest (between mid-May and end of September, Figure 3).

Evaporative enrichment of the soil water isotopes, given as lc-excess, was highest and most dynamic in the top soil (Figure 2, Figure S3). The lc-excess usually decreased with soil depth leading to regression lines in the dual isotope space with varying slopes over the seasons and among sampling locations (Figure 4). The slopes of these regression lines were generally lower than the slopes of the LMWL. The relationship between the average lc-excess in the upper 30 cm of soil and the average PET over 30 days prior to the sampling (PET_{30}) revealed that the lc-excess was not necessarily lowest during highest evaporative demand (summer), but lc-excess was lowest after the peak PET_{30} (Figure 5). Thus, soil waters were still highly fractionated just before the dormant season started. These patterns in lc-excess dynamics indicate that there is a memory effect regarding the evaporation fractionation in the soil waters. The relationship between lc-excess and PET_{30} was not necessarily linear, but there was a time lag with spring

sampling campaigns often resulting in highest lc-excess (closest to the slope of the LMWL as shown in Figure 4), even though PET_{30} values were already as high as during the autumn samples (Figure 5).

3.1.2 Variability across sampling locations

Average soil water δ^2H and $\delta^{18}O$ values of the upper 30 cm at each sampling location could not be explained in terms of corresponding antecedent temperature T_{30}, evaporative demand PET_{30} or VSM ($r < 0.14$, not shown). Antecedent precipitation volumes P_{30} showed significant correlation with soil water δ^2H and $\delta^{18}O$ values across locations ($r = 0.66$ and $r = 0.58$, respectively). However, the relatively dry summers in Wolf Creek and Dry Creek (relative to the wetter locations at Bruntland Burn, Dorset and Krycklan), where the depleted snow melt and spring precipitation is stored in the soil over the summer, appear to drive this relationship, rather than a causal relationship between precipitation volumes and soil water isotopes.

Average soil water lc-excess in the upper 30 cm at the sampling locations generally correlated significantly with corresponding P_{30} and T_{30} (Figure 6). When limiting the data to spring, none of the predictors showed a significant correlation with soil water lc-excess. For the summer sampling dates, only P_{30} showed a significant relationship with soil water lc-excess, while the lc-excess of autumn samples had a significant correlation to P_{30} and T_{30}. VSM did not show a significant linear relationship with soil water lc-excess (Figure 6).

To assess the relative importance of controlling variables potentially explaining the soil water lc-excess across the sampling locations, multiple linear regression was applied to the pooled data sets. Results showed that P_7 explained 100 % of the variation in soil water lc-excess when all data was considered(Table 3). Soil water lc-excess during spring was mainly explained by P_7 (81%) and partially by T_{30} (19%). 83 % of soil water lc-excess variability during summer could

be explained by P_{30}, while T_{30} explained 17 %. Most important in explaining the soil water lc-excess in autumn was the combined effect of T_{30} and VSM (35 %) and both P_{30} and T_{30} explained about 26 %, while VSM accounted for 9 % and the combination of P_{30} and T_{30} explained just 3 % (Table 3). Using logarithmic or exponential transformations for the multiple linear regression did not improve the regression fit.

3.2 Effects of vegetation

Vegetation cover had a significant effect on the soil water isotopic composition at the Bruntland Burn sampling locations, which were of similar soil texture. Soil water beneath Scots pine was generally more enriched in heavy isotopes (median ± standard deviation δ^2H = -50.9 ± 10.6 ‰, lc-excess = -3.6 ± 4.7‰) than soil water beneath heather (δ^2H = -52.4 ±9.9‰, lc-excess = -2.3±3.6‰). The vegetation effect on soil water δ^2H was statistically significant in the upper 10 cm, where 80 to 90 % of the fine roots are located (Figure 7a). Regarding the lc-excess, the evaporation signal was significantly more pronounced beneath Scots pine compared to soils beneath heather, across the upper 15 cm of the profile (Figure 7b).

At Dorset, the soil water δ^2H beneath broad-leaved trees (Red oaks, δ^2H = -52.2±12.1 ‰) were not significantly different to soil water beneath conifer trees (δ^2H: -53.4±10.6 ‰) and soil water δ^2H did not show a consistent pattern in the comparison between the two landscape units across the soil profile (Figure 7c). However, the soil water lc-excess in the upper 50 cm was significantly lower beneath conifers (lc-excess = -4.1±6.3 ‰) than beneath broad-leaved trees (lc-excess: -2.0±6.5 ‰). The lc-excess values were consistently more negative beneath the conifers across the soil profile, but significant differences were limited to 10-15, 15-20, and 25-30 cm sampling depths (Figure 7d).

3.3 Effect of topography

Soil waters of sampling locations in the riparian zone at Krycklan and Wolf Creek were generally more depleted in heavy isotopes compared to the nearby upslope locations. Soil waters at S04 were significantly more depleted in δ^2H (-88.2±5.1 ‰) than at S22 (δ^2H = -80.5±8.4 ‰). The soil water isotopes at S04 were more depleted and of lower variability at all sampled depths compared to S22 (Figure 8a). In terms of lc-excess values, the soil waters at S04 and S22 did not differ significantly; neither for the entire upper 30 cm (lc-excess = -0.6±2.3 ‰ and lc-excess = -0.9±2.8 ‰, respectively), nor for any depth of the sampled profiles, with the exception of 20-30 cm (Figure 8b).

At Wolf Creek, RP was significantly more depleted in its soil water δ^2H composition (-159.8±8.8 ‰) compared to the PL location (δ^2H = -154.6±11.2 ‰). The differences across the soil profile were significant for the 30-40 cm depth interval, but the PL median soil water δ^2H values were generally more enriched across the entire profile and showed higher variability (Figure 8c). Similar to the Krycklan locations, the soil water lc-excess did not differ significantly (PL lc-excess -5.5±15.2 ‰ and RP lc-excess -8.3±13.7 ‰) across the upper 40 cm nor at any particular depth.

3.4 Effect of elevation

Soil water isotopes at the lower elevation site in Dry Creek, LG, were significantly more enriched in heavy isotopes than the higher elevation site at tree line, TL (δ^2H = -118.1±12.4 ‰ and δ^2H = -125.3±14.1 ‰, respectively). Across the soil profile, the TL soil waters were consistently depleted in δ^2H compared to LG, but these differences were not statistically significant (Figure 9a). However, the soil water lc-excess values were generally significantly

different between the two locations, with median values of -15.0±17.0 ‰ at the LG location and -8.5±17.7 ‰ at TL. Median lc-excess values at each sampled soil depth were more negative at LG than at TL (Figure 9b).

3.5 Mixing processes in the subsurface

We infer mixing processes from correlation analysis between soil water δ^2H (δ_{SW}) dynamics and weighted averages of the precipitation/snow melt δ^2H signal prior to the sampling (δ_P). The relationship between δ_{SW} and δ_P generally decreased with depth at Bruntland Burn, Dorset, Krycklan, and Wolf Creek (Figure 10). There was usually no correlation of δ_{SW} with the most recent infiltrated water (P_2). Also the infiltrating water over a week prior to the soil water sampling showed little correlation with δ_{SW} and was often limited to the upper 5 to 10 cm. At Bruntland Burn and S22, correlation between δ_{SW} and δ_{P30} was generally high ($r > 0.6$). However, at the S04 location, this relationship decreased sharply within the upper 20 cm and was absent ($r = 0$) at 20-30 cm depth. At the Dorset locations and PL at Wolf Creek, the relationship between stable isotopic composition in precipitation and soil water dropped below 25 cm soil depth. At Wolf Creek RP and the Dry Creek locations, no relationship between antecedent precipitation input and soil water response was evident.

These correlation analyses reveal that the soil waters were mainly composed of a mixture of older (more than two weeks) infiltrated waters. This is supported by the relatively low slopes of the regression between δ_{SW} and δ_{P30}. The soil water isotopic compositions were generally more depleted in heavy isotopes than the infiltrating water ($m < 1$), which means that the soils pore waters were dominated by isotopically depleted water infiltrated during winter or snow melt. For all sites, this regression slope generally decreased over the upper 30 cm soil depth (Figure 10).

At the top 5 cm of soil at the Bruntland Burn locations, the soil waters were closest to P_{30}, while the riparian zone locations, very rich in organic material, had generally low regression slopes between δ_{SW} and δ_{P30}. (S04 between 0.2 and 0; RP about zero). Also at Dry Creek, where very little precipitation falls during summer and autumn, the slopes were close to zero, but partly <0.

4 Discussion

4.1 Hydro-meteorological controls on the stable isotopic composition of soil waters

Our results for the northern latitudes underline that the soil-vegetation-atmosphere interface is a crucial area that needs to be incorporated at sufficiently fine resolution in soil water sampling designs to understand water transport and mixing processes through the critical zone. As all sites at the long-term experimental catchments had a significantly different soil water δ^2H (and $\delta^{18}O$) signal in the top 10 cm compared to the soil waters below 10 cm, our study highlights the importance of the upper critical zone as an important interface. The sampling depths and sampling intervals over depth strongly influenced the interpretation of the soil water isotope data, since intense interactions between soil, vegetation and atmosphere take place in the upper critical zone. Our results showed that isotopic fractionation in the bulk soil water was highest within the top 10 cm of the soil, which has important implications for ecohydrological studies when relating the isotopic compositions of soil waters to plant waters to estimate root water uptake depths (see review by Rothfuss and Javaux (2017)). Missing the highly fractionated soil waters of the top soil, where fine root densities are often highest (Jackson et al., 1996; Zeng, 2001), can potentially lead to misinterpretations in ecohydrological studies. As previously shown for Dry Creek and Bruntland Burn, the isotope fractionation (lc-excess < 0) can reach down to 70 cm (McCutcheon et al., 2016) or be limited to the upper 15 cm (Sprenger et al., 2017a), respectively. However, an

explanation of the temporal variability of the soil water lc-excess signal at the individual catchments was impeded by the limited range of both the soil water isotopic signals and the explanatory variables at each of the sites (Table S1).

Our study, therefore, benefitted from the unique data setof several sampling locations of varying hydro-meteorological conditions, which provided an opportunity to analyse the factors driving the temporal variability of soil water fractionation signals. While soil water δ^2H and $\delta^{18}O$ values were generally related to the respective input signal of precipitation, the dual isotope approach of using the lc-excess that describes the ratio between δ^2H and $\delta^{18}O$ revealed new insights into the isotopic fractionation due to soil evaporation. In line with findings by Hsieh, Chadwick, Kelly, and Savin (1998), the kinetic fractionation of stable isotopes in soil water was negatively correlated with precipitation sums and positively correlated with potential evaporation rates. However, our multiple linear regression analysis revealed the relative importance of different explanatory variables. We found that neither potential evaporation (PET_{30}) nor air temperature (T_{30}) were the most important factors to explain the lc-excess variability over time and space at the different sampling locations. Instead, antecedent precipitation (P_7) explained the variability of soil water lc-excess values for the entire data set. Also for the spring and summer sampling campaigns, the recent infiltration volumes (P_7) for spring and the infiltration over the previous month (P_{30}) for summer were with 80 % the most important factors. Thus, while soil evaporation is necessary for kinetic fractionation of the soil water (lc-excess < 0), the fractionation signal will be diluted by newly un-fractionated precipitation input (lc-excess = 0). Such a dependency of the fractionation signal on precipitation input was also shown for bulk soil waters in south-central Chile, where the soil water lc-excess values approached zero during the rainy season (Hervé-Fernández et al., 2016).

Soil moisture only affected the lc-excess signal for the autumn sampling campaigns. Therefore, when evaporation rates decreased and little further fractionation took place in autumn, the volume of the stored water had an influence on the evaporation signal of the stable isotope compositions: The dilution of the evaporation signal established mainly during summer is slower for soils that have higher soil moisture contents in autumn. That the dilution of the isotopic fractionation signal took time - or more appropriately, needed more cumulative precipitation input – is shown by the fact that the lc-excess of the soil waters in the upper 30 cm were lowest after the peak evaporation at all sites (Figure 5). Thus, the soil water isotopic fractionation dynamics lagged the evaporation dynamics, resulting in a "memory effect" in the soil water of the upper layer. Our data therefore supports recent theoretical considerations by Benettin et al. (2018) that soil water isotopic compositions are most fractionated in autumn due to mixing of waters. This has important implications for ecohydrological studies, as this implies that the soil water is highly enriched during the plant water uptake just before dormancy of the vegetation. This could potentially explain isotopically enriched xylem waters sampled after dormancy, as presented by McCutcheon et al. (2016). Due to the interplay between transient soil moisture content, fractionating evaporation output and fractionation-diluting precipitation input, there is no linear relation between soil evaporation and the kinetic fraction signal of the bulk soil waters. This lagged response of the bulk soil waters, not only to precipitation/snow melt infiltration, but also soil evaporation losses, is in strong contrast to the relatively quick response in the waters of the more mobile water, sampled with suction lysimeters at Bruntland Burn, Dorset, and Krycklan (Sprenger, Tetzlaff, Buttle, Laudon, Leistert et al., 2018). Thus, an ecohydrological separation, where mobile soil waters are isotopically different from bulk soil waters (Brooks, Barnard, Coulombe, & McDonnell, 2010), is probably linked to different water ages. As our results show,

the soil pores between 5 and 25 cm depth are usually composed of waters older than at least two weeks and will therefore be obviously different from recently infiltrated water, sampled with suction lysimeters. Latest simulations with a soil physical model underlined that the median water ages in the upper 10 cm of soil at the Bruntland Burn, Dorset and Krycklan sites vary between few days and up to 50 days during the growing season (Sprenger, Tetzlaff, Buttle, Laudon, & Soulsby, 2018).

4.2 The role of vegetation, topography and elevation for storage, mixing and flux of water in the critical zone

The soil water isotope data from the five different catchments provide insights into some of the ways how the vegetation cover, topography and elevation influence the soil water isotope composition. Regarding the vegetation influences found at Bruntland Burn and Dorset, the impact of an altered infiltration signal due to isotopic fractionation of the throughfall can be excluded as a comparison between stable isotopes of throughfall and gross rainfall did not show a significant offset at these sites (Soulsby, Braun, Sprenger, Weiler, & Tetzlaff, 2017, Snelgrove, unpublished data, 2017). As isotopic fractionation was generally higher for the soil waters beneath the Scots pines compared to the soils beneath heather at Bruntland Burn, these differences can be related to less dense canopy cover, lower humidity, and higher soil-atmosphere vapor exchange in the forest (Sprenger et al., 2017a). Similarly, Zhang, An, Xu, Cui, and Xu (2011) also related higher atmospheric humidity due to vegetation cover to decreased isotopic fractionation of soil waters. At Dorset, lc-excess was lower beneath the coniferous trees than beneath the broadleaf Red oak, despite limited differences between the two vegetation types in terms of canopy cover. However, the vegetation influence on the evaporation signal at both Bruntland Burn and Dorset sites was limited to the top soil with no significant differences below 15 cm and 30 cm, respectively. Thus, variability of the isotopic signal across the soil profile was

most intense in the upper layers of the unsaturated zone where the soil-vegetation-atmosphere interactions take place.

The topographic influences between hillslope and riparian zone on δ^2H values were consistent at Krycklan and Wolf Creek. At both catchments, soil waters closer to the stream were less variable and generally more depleted in δ^2H compared to the soil water on the hillslopes. These findings indicate greater mixing of different flow paths and waters of different ages in the subsurface towards the riparian zone, confirming their "isostat" behaviour described in Tetzlaff, Birkel, Dick, Geris, and Soulsby (2014). This interpretation corresponds with other studies where a lower variability of the stable isotope composition in soil waters in time (Asano, Uchida, & Ohte, 2002) or over the soil depth (Garvelmann, Külls, & Weiler, 2012) was associated with greater mixing towards the stream. In fact, isotopic composition of soil waters at the riparian zone locations, S04 and RP, appeared to be disconnected from the isotopically variable precipitation input ($r < 0.2$ below 15 cm soil depth, Figure 10). Since the δ^2H values at these locations are generally more depleted than the incoming precipitation (regression slopes δ^2_{SW} and δ^2_{P30} <0.2, Figure 10), we saw that depleted winter precipitation or snow melt is preferably recharging the riparian zone. Hence, seasonal root water uptake during the growing season affects the long-term isotope balance of the critical zone, which eventually governs the groundwater isotopic composition (slightly above the LMWL, Figure 4). Additionally, the high organic matter content at S04 and RP results in high pore volumes, which affect the mixing processes in the riparian soils.

Our soil water samples at the plot scale support the interpretation of catchment scale isotope studies in northern latitudes and/or regions with snow cover that the most intense recharge of groundwater occurs from waters depleted in heavy isotopes such as snow melt (Dry Creek,

Dorset, Krycklan, Wolf Creek) and winter rainfall (Bruntland Burn) (Jasechko, Wassenaar, & Mayer, 2017; Scheliga, Tetzlaff, Nuetzmann, & Soulsby, 2017; Sprenger, Tetzlaff, Tunaley, Dick, & Soulsby, 2017; Zapata-Rios et al., 2015). At Dry Creek, the soil pores get filled during the snow melt in early spring and this melt water stays in the soil over the summer, since little precipitation occurs then. Therefore, stable isotopic composition does not show a relationship to the isotopic composition of antecedent precipitation input (Figure 10). Because of this intense seasonality of precipitation/snow melt input at Dry Creek, mixing of soil waters with newly introduced precipitation during summer is little, leading to high fractionation of the isotopes in the soil water (Figure 3). Our data from northern environments showed no differences between soil waters in the riparian zone and the hillslope regarding their evaporation fractionation signal. In contrast, Simonin et al. (2014) showed that the uppermost (0-5 cm) soil layer was more isotopically fractionated at the hillslopes compared to the valley bottom in a Mediterranean environment.

The effect of elevation on the isotopic signal of precipitation is well documented (e.g., Ambach, Dansgaard, Eisner, & Moller, 1968) and this altitude effect for the Dry Creek catchment was approximately 1.8 ‰ depletion in δ^2H per 100 m elevation (Tappa, Kohn, McNamara, Benner, & Flores, 2016). This difference of the precipitation input signal between LG and TL is reflected in the soil water δ^2H depth profiles (Figure 9a). The lc-excess depth profiles are significantly different for the two sampling locations, with higher fractionated isotopic composition at the lower sampling location indicating higher soil evaporation losses. Due to the extended dry periods and relatively high temperatures during summer, the soil water fractionation extends to 70 cm depth. Therefore, contrary to the effect of vegetation, the elevation effect is not limited to the upper 30 cm, but results in significant differences in lc-excess values through the deeper soil

profile. We explain these differences in soil water lc-excess in terms of longer snow free periods, higher evaporation, and less precipitation at LG compared to TL (Table 1).

The various controls on the soil water isotopic composition emphasise the spatial in addition to the temporal variability in δ^2H, $\delta^{18}O$, and lc-excess of waters within the critical zone. These varying isotopic signals result from different processes such as increased mixing along longer flow paths (advection-dispersion) or soil evaporation in varying landscape units. Such information can be used to calibrate (Sprenger, Seeger et al., 2016) or validate (Mueller et al., 2014) water flow and transport simulations with soil physical models at the profile or the hillslope scale (Windhorst, Kraft, Timbe, Frede, & Breuer, 2014). Stable isotope data of the water in the critical zone of representative landscape units can further increase the physical realism of spatially distributed tracer-aided catchment models (Soulsby et al., 2015; van Huijgevoort, Tetzlaff, Sutanudjaja, & Soulsby, 2016). Regarding such modelling approaches, crucially, the presented data can also help to assess water age dynamics in the critical zone, as the dampening of the highly variable precipitation isotope compositions over the soil depth can be related to the travel time (DeWalle, Edwards P.J., Swistock B.R., Aravena R., & Drimmie R.J, 1997). It has been shown in several studies that this damping happens mostly within the upper 30 cm (reviewed in Sprenger, Leistert et al., 2016). Usually, the isotopic signal of mobile water (sampled with lysimeters) is used for travel time analysis in the soil (e.g., Muñoz-Villers & McDonnell, 2012; Tetzlaff et al., 2014; Timbe et al., 2014). The data presented here are bulk soil water isotopes including pore waters of potentially older ages compared to mobile waters that were shown to have only little to no isotopic fractionation at Bruntland Burn (Geris, Tetzlaff, McDonnell, & Soulsby, 2015), Dorset (Sprenger, Tetzlaff, Buttle, Laudon, Leistert et al., 2018) and Krycklan (Peralta-Tapia, Sponseller, Tetzlaff, Soulsby, & Laudon, 2015). Considering the

above discussed impacts of vegetation, topography and elevation on the bulk soil water isotopic compositions, we can expect that such processes will affect the age dynamics of the soil waters, resulting in different travel time estimates than limiting the analysis to the mobile water phase (Sprenger, Tetzlaff, Buttle, Laudon, & Soulsby, 2018).

5 Conclusion

Stable isotope data of bulk soil waters at various locations in five catchments spanning a wide range of hydro-meteorological conditions in northern latitude environments, provided a unique insight into storage, mixing and release of waters within the upper critical zone. We showed the benefits of examining a suite of data sets to cover a wider range of both response variables (e.g. lc-excess in top 30 cm) and predictors (e.g., P_7, P_{30}, T_{30}, VSM). While it is expected that higher temperatures lead to higher soil evaporation that kinetically fractionates the soil water isotopes, mixing with infiltrated precipitation that is un-fractionated was found to be the dominant driver of the soil water lc-excess signal amongst the 14 sampling locations. The resulting memory effect in the isotopic compositions results in an evaporation fractionation of soil waters that is most intense during autumn. The observed lag between isotopic evaporation signal in the soil water and the evaporation rates lead to pronounced isotopic fractionation signals in the soil just before vegetation dormancy. This can have important consequences for the interpretation of ecohydrological studies relating the isotopic composition of soil and vegetation water dependent on the timing and frequency of the sampling: Our findings underscore the need of sampling the shallow soils as they are most dynamic as well as considering the seasonal variability of soil water isotope compositions and their hydro-meteorological drivers.

We further showed that there are common effects of vegetation cover on the evaporation signal of soil water with more pronounced differences between soils beneath Scots pine and heather

than between conifers and Red oaks. Topography was also found to affect soil water isotopes, indicating more mixing and greater contributions of older water towards stream channels. However, also in shallow soil layers, the presented bulk water generally comprised waters older than 14 days. This indicates that the pore water is usually not fully replaced by recent infiltration events, but bulk and mobile soil waters are probably of different isotopic composition and thus represent different water ages. In general, integration of such spatially variable stable isotope data can help resolve the partitioning of precipitation in the upper soil zone and improve estimates of travel times or root water uptake depths of the critical zone.

Acknowledgements

We thank Audrey Innes for isotope analysis at University of Aberdeen for Bruntland Burn and Krycklan sites, Johannes Tiwari (SLU) for isotope sampling in Krycklan, Pernilla Löfvenius (SLU) for providing PET data for Krycklan (via SITES), and Jeff McDonnell and Kim Janzen (University of Saskatchewan) for soil water isotope analysis for the Dorset and Wolf Creek sites. The Krycklan part was funded by the KAW Branch-Point project. We acknowledge the funding from the European Research Council (ERC, project GA 335910 VeWa). We thank the Editor and three anonymous reviewers for their critical comments during the peer-review process.

Figures

Figure 1 Map of each of the five long-term experimental catchments showing the soil sampling (black stars) locations, the elevation and the rivers. The location of each catchment is indicated with the points on the world map (taken from: https://commons.wikimedia.org).

Figure 2 Dual isotope plots showing precipitation (left) and soil water (right) isotope data at the five long-term experimental catchments (colour code). The soil water samples are split into samples taken in the upper 10 cm (shown in dark with black contour colours in box plots and as triangles in dual isotope plot) and below 10 cm (bright colours in box with grey lines in box plots and circles in dual isotope plot). Note that the samples in the upper 10 cm for all sites are significantly more enriched in heavy isotopes compared to the samples below (Mann-Whitney-U test, $p < 0.05$).

Figure 3 Soil water lc-excess between mid-May and end of September (growing season at the study sites) for each site divided into samples from the upper 10 cm (black lines and dark colours) and below 10 cm soil depth (bright colours and grey lines). The stars indicate significant differences between the subset at each site (Mann-Whitney-U test, $p<0.05$).

Figure 4 Dual isotope plot for each study site showing all soil water samples for different seasons (colour code). Regression lines through the samples for each sampling day are shown. Black lines show the GMWL and the dashed lines show the LMWL for the individual catchments. Black squares indicate the long-term groundwater signal (no data for Dorset).

Figure 5 Time series of the average potential evapotranspiration over the 30 days prior to the sampling (PET_{30}, dashed lines) and the average lc-excess of the soil samples in the upper 30 cm. All data are unity-based normalized to get values between 0 (minimum value) and 1 (maximum

value). Note that the axis of lc-excess is inverted and that a smaller value of lc-excess indicates higher kinetic fractionation.

Figure 6 Relationship between soil water lc-excess signal in the upper 30 cm of soil with the precipitation sum over 30 days prior to each sampling (P_{30}, 1st column), the average temperature over the 30 days prior each sampling (T_{30}, 2nd column), and the volumetric soil moisture (VSM, 3rd column) for all samples (1st row) and for the samples taken in spring (2nd row), summer (3rd row), and autumn (4th row). Colours represent the catchments and the marker style represent the sampling locations within individual catchments. Coefficient of determinations (r^2) are given, linear best-fit lines are shown for significant regressions ($p < 0.05$) and locally weighted regressions (LOWESS filter) are plotted as dashed line.

Figure 7 Effects of vegetation on the soil water isotopes with examples from Bruntland Burn (a and b) and Dorset (c and d). Points represent the individual samples and the violin plots show the distribution as a kernel density estimation of the soil water (a and c) δ^2H and (b and d) lc-excess. The vertical dashed lines within the violin plots represent the 25th, 50th, and 75th quartiles. "X" next to the violin plots indicates significant differences between vegetation types (Paired Wilcoxon rank sum test, $p < 0.05$).

Figure 8 Effects of topography on soil water isotopes with example from Krycklan (a) and b)) and Wolf Creek (c) and d)). Points represent the individual samples and the violin plots show the distribution as a kernel density estimation of the soil water (a and c) δ^2H and (b and d) lc-excess. The vertical dashed lines within the violin plots represent the 25th, 50th, and 75th quartiles. "X" next to the violin plots indicates significant differences between slope positions (Paired

Wilcoxon rank sum test, $p < 0.05$). Note, for Wolf Creek, only sampling days in parallel were considered and depth intervals were constructed.

Figure 9 Effects of altitude on soil water isotopes with example from Dry Creek. Points represent the individual samples and the violin plots show the distribution as a kernel density estimation of the soil water (a) δ^2H and (b) lc-excess. The vertical dashed lines within the violin plots represent the 25^{th}, 50^{th}, and 75^{th} quartiles. "X" next to the violin plots indicates significant differences between altitudes (Paired Wilcoxon rank sum test, $p < 0.05$).

Figure 10 Correlation coefficient *r* of the relationship between the soil water δ^2H at different depths and the 2-, 7-, 14-, and 30-day weighted average precipitation or snowmelt δ^2H input (P_2, P_7, P_{14}, P_{30}, respectively). For P_{30}, also the slope of the regression between soil water δ^2H and P_{30} is given. The color code represents the scale between -1 and 1 as given in the color bar on the bottom left.

Tables

Table 1 Environmental characteristics of each study site: Average values of precipitation sum (P), air temperature (T), potential evapotranspiration (PET), and number of dry days for 12 months during the sampling period (Table 2); soil type, soil texture description, vegetation cover, elevation and groundwater depth at the sampling locations within the five long-term experimental catchments. OM = organic matter content.

Table 2 Isotope sampling design (number of sampling campaigns, sampling period, maximum sampling depth, and total sample number), mean volumetric soil moisture at 10 cm (VSM) and isotopic characteristics of the precipitation (P) and soil waters in the upper 30 cm.

Table 3 Results of multiple linear regression models to explain the soil water lc-excess data pooled for each sampling site over different time periods: all available data, spring, summer, and autumn (as shown in Figure 6). The significance level for each parameter is given according to ANOVA of the linear models. *** = $p<0.001$; **=$p<0.01$; *=$p<0.05$, •=$p<0.10$, n.s. indicates parameters that were not significant for the model. Percentage in brackets show the relative importance of the explanatory parameter. Note that the lc-excess data was reciprocally transformed for "All data" and "Summer" to get normal distributions and that the lc-excess of the samples taken in autumn was not normally distributed.

6 References

Allen, R. G., Pereira, L. S., Raes, D., & Smith, M. (1998). Crop evapotranspiration-Guidelines for computing crop water requirements-FAO Irrigation and drainage paper 56. *FAO, Rome*, *300*(9), D05109.

Ambach, W., Dansgaard, W., Eisner, H., & Moller, J. (1968). The altitude effect on the isotopic composition of precipitation and glacier ice in the Alps. *Tellus*, *20*(4), 595–600. https://doi.org/10.1111/j.2153-3490.1968.tb00402.x

Asano, Y., Uchida, T., & Ohte, N. (2002). Residence times and flow paths of water in steep unchannelled catchments, Tanakami, Japan. *Journal of Hydrology*, *261*(1-4), 173–192. https://doi.org/10.1016/S0022-1694(02)00005-7

Benettin, P., Volkmann, T. H. M., Freyberg, J. von, Frentress, J., Penna, D., Dawson, T. E., & Kirchner, J. W. (2018). Effects of climatic seasonality on the isotopic composition of evaporating soil waters. *Hydrol. Earth Syst. Sci. Discuss.*, 1–16. https://doi.org/10.5194/hess-2018-40

Brooks, J. R., Barnard, H. R., Coulombe, R., & McDonnell, J. J. (2010). Ecohydrologic separation of water between trees and streams in a Mediterranean climate. *Nature Geoscience*, *3*(2), 100–104. https://doi.org/10.1038/NGEO722

Brooks, P. D., Chorover, J., Fan, Y., Godsey, S. E., Maxwell, R. M., McNamara, J. P., & Tague, C. (2015). Hydrological partitioning in the critical zone: Recent advances and opportunities for developing transferrable understanding of water cycle dynamics. *Water Resources Research*, *51*(9), 6973–6987. https://doi.org/10.1002/2015WR017039

Clark, M. P., Schaefli, B., Schymanski, S. J., Samaniego, L., Luce, C. H., Jackson, B. M., Freer, J. E., Arnold, J. R., Moore, R. D.,. . . Ceola, S. (2016). Improving the theoretical underpinnings of process-based hydrologic models. *Water Resources Research*, *52*(3), 2350–2365. https://doi.org/10.1002/2015WR017910

Cleveland, W. S. (1979). Robust locally weighted regression and smoothing scatterplots. *Journal of the American statistical association*, *74*(368), 829–836.

Coplen, T. B. (2011). Guidelines and recommended terms for expression of stable-isotope-ratio and gas-ratio measurement results. *Rapid Communications in Mass Spectrometry*, *25*(17), 2538–2560. https://doi.org/10.1002/rcm.5129

DeWalle, D.R., Edwards P.J., Swistock B.R., Aravena R., & Drimmie R.J. (1997). Seasonal isotope hydrology of three Appalachian forest catchments. *Hydrological Processes*, *11*, 1895–1906. https://doi.org/10.1002/(SICI)1099-1085(199712)11:15<1895::AID-HYP538>3.0.CO;2-#

Evaristo, J., Jasechko, S., & McDonnell, J. J. (2015). Global separation of plant transpiration from groundwater and streamflow. *Nature*, *525*(7567), 91–94. https://doi.org/10.1038/nature14983

Fenicia, F., Wrede, S., Kavetski, D., Pfister, L., Hoffmann, L., Savenije, H. H. G., & McDonnell, J. J. (2010). Assessing the impact of mixing assumptions on the estimation of streamwater mean residence time. *Hydrological Processes*, *24*(12), 1730–1741. https://doi.org/10.1002/Hyp.7595

Garvelmann, J., Külls, C., & Weiler, M. (2012). A porewater-based stable isotope approach for the investigation of subsurface hydrological processes. *Hydrology and Earth System Sciences*, *16*(2), 631–640. https://doi.org/10.5194/hess-16-631-2012

718 Gat, J. R., & Gonfiantini, R. (Eds.). (1981). *Stable Isotope Hydrology: Deuterium and Oxygen-*
719 *18 in the Water Cycle*. *Technical Report Series*. Vienna, Austria: IAEA.
720 Geris, J., Tetzlaff, D., McDonnell, J., Anderson, J., Paton, G., & Soulsby, C. (2015).
721 Ecohydrological separation in wet, low energy northern environments? A preliminary
722 assessment using different soil water extraction techniques. *Hydrological Processes*, *29*(25),
723 5139–5152. https://doi.org/10.1002/hyp.10603
724 Geris, J., Tetzlaff, D., McDonnell, J., & Soulsby, C. (2015). The relative role of soil type and
725 tree cover on water storage and transmission in northern headwater catchments. *Hydrological*
726 *Processes*, *29*(7), 1844–1860. https://doi.org/10.1002/hyp.10289
727 Geris, J., Tetzlaff, D., McDonnell, J. J., & Soulsby, C. (2017). Spatial and temporal patterns of
728 soil water storage and vegetation water use in humid northern catchments. *The Science of the*
729 *total environment*, *595*, 486–493. https://doi.org/10.1016/j.scitotenv.2017.03.275
730 Grant, G. E., & Dietrich, W. E. (2017). The frontier beneath our feet. *Water Resources Research*,
731 *53*(4), 2605–2609. https://doi.org/10.1002/2017WR020835
732 Grömping, U. (2006). Relative Importance for Linear Regression in R: The Package relaimpo.
733 *Journal of Statistical Software*, *17*(1). https://doi.org/10.18637/jss.v017.i01
734 Hartmann, D. L., Klein Tank, A.M.G., Rusticucci, M., Alexander, L. V., Brönnimann, S.,
735 Charabi, Y., Dentener, F. J., Dlugokencky, E. J., Easterling, D. R.,. . . Zhai, P. M. (2013).
736 Observations: Atmosphere and Surface. In T. F. Stocker, D. Qin, G.-K. Plattner, M. Tignor, S.
737 K. Allen, J. Boschung,. . . P. M. Midgley (Eds.), *Climate Change 2013: The Physical Science*
738 *Basis.: Contribution of Working Group I to the Fifth Assessment Report of the*
739 *Intergovernmental Panel on Climate Change.* Cambridge, United Kingdom and New York,
740 NY, USA: Cambridge University Press.

Hendry, M. J., Schmeling, E., Wassenaar, L. I., Barbour, S. L., & Pratt, D. (2015). Determining the stable isotope composition of pore water from saturated and unsaturated zone core: improvements to the direct vapour equilibration laser spectrometry method. *Hydrol. Earth Syst. Sci.*, *19*(11), 4427–4440. https://doi.org/10.5194/hess-19-4427-2015

Hervé-Fernández, P., Oyarzún, C., Brumbt, C., Huygens, D., Bodé, S., Verhoest, N. E. C., & Boeckx, P. (2016). Assessing the "two water worlds" hypothesis and water sources for native and exotic evergreen species in south-central Chile. *Hydrological Processes*, *30*(23), 4227–4241. https://doi.org/10.1002/hyp.10984

Hollander, M., & Wolfe, D. A. (1973). *Nonparametric Statistical Methods*. New York: John Wiley & Sons.

Holm, S. (1979). A simple sequentially rejective multiple test procedure. *Scandinavian Journal of Statistics*, *6*, 65–70.

Holtmeier, F.-K., & Broll, G. (2005). Sensitivity and response of northern hemisphere altitudinal and polar treelines to environmental change at landscape and local scales. *Global Ecology and Biogeography*, *14*(5), 395–410. https://doi.org/10.1111/j.1466-822x.2005.00168.x

Hsieh, J. C. C., Chadwick, O. A., Kelly, E. F., & Savin, S. M. (1998). Oxygen isotopic composition of soil water: Quantifying evaporation and transpiration. *Geoderma*, *82*(1–3), 269–293. https://doi.org/10.1016/S0016-7061(97)00105-5

Jackson, R. B., Canadell, J., Ehleringer, J. R., Mooney, H. A., Sala, O. E., & Schulze, E. D. (1996). A global analysis of root distributions for terrestrial biomes. *Oecologia*, *108*(3), 389–411. https://doi.org/10.1007/BF00333714

Jasechko, S., Wassenaar, L. I., & Mayer, B. (2017). Isotopic evidence for widespread cold-season-biased groundwater recharge and young streamflow across central Canada. *Hydrological Processes*, *31*(12), 2196–2209. https://doi.org/10.1002/hyp.11175

Kottek, M., Grieser, J., Beck, C., Rudolf, B., & Rubel, F. (2006). World Map of the Köppen-Geiger climate classification updated. *Meteorologische Zeitschrift*, *15*(3), 259–263. https://doi.org/10.1127/0941-2948/2006/0130

Landwehr, J. M., & Coplen, T. B. (2006). Line-conditioned excess: a new method for characterizing stable hydrogen and oxygen isotope ratios in hydrologic systems. In *International Conference on Isotopes in Environmental Studies* (pp. 132–135). Vienna: IAEA.

Maher, K. (2010). The dependence of chemical weathering rates on fluid residence time. *Earth and Planetary Science Letters*, *294*(1-2), 101–110. https://doi.org/10.1016/j.epsl.2010.03.010

Majoube, M. (1971). Fractionnement en oxygene-18 et en deuterium entre l'eau et sa vapeur. *J. Chim. phys*, *68*(10), 1423–1436.

McCutcheon, R. J., McNamara, J. P., Kohn, M. J., & Evans, S. L. (2016). An Evaluation of the Ecohydrological Separation Hypothesis in a Semiarid Catchment. *Hydrological Processes*, *31*(4), 783–799. https://doi.org/10.1002/hyp.11052

McDonnell, J. J., & Beven, K. (2014). Debates-The future of hydrological sciences: A (common) path forward? A call to action aimed at understanding velocities, celerities and residence time distributions of the headwater hydrograph. *Water Resources Research*, *50*(6), 5342–5350. https://doi.org/10.1002/2013WR015141

McMillan, H. K. (2012). Effect of spatial variability and seasonality in soil moisture on drainage thresholds and fluxes in a conceptual hydrological model. *Hydrological Processes*, n/a. https://doi.org/10.1002/hyp.9396

Mueller, M. H., Alaoui, A., Kuells, C., Leistert, H., Meusburger, K., Stumpp, C., Weiler, M., & Alewell, C. (2014). Tracking water pathways in steep hillslopes by $\delta^{18}O$ depth profiles of soil water. *Journal of Hydrology*, *519*(A), 340–352. https://doi.org/10.1016/j.jhydrol.2014.07.031

Muñoz-Villers, L. E., & McDonnell, J. J. (2012). Runoff generation in a steep, tropical montane cloud forest catchment on permeable volcanic substrate. *Water Resources Research*, *48*(9), W09528. https://doi.org/10.1029/2011WR011316

Orlowski, N., Pratt, D., Breuer, L., & McDonnell, J. J. (2017). Critical Evaluation of Soil Pore Water Extraction Methods on a Natural Soil. In European Geoscience Union (Ed.): *Vol. 19. Geophysical Research Abstracts, EGU General Assembly 2017* (EGU2017-9905). Vienna.

Peralta-Tapia, A., Soulsby, C., Tetzlaff, D., Sponseller, R., Bishop, K., & Laudon, H. (2016). Hydroclimatic influences on non-stationary transit time distributions in a boreal headwater catchment. *Journal of Hydrology*, *543*(Part A), 7–16. https://doi.org/10.1016/j.jhydrol.2016.01.079

Peralta-Tapia, A., Sponseller, R. A., Tetzlaff, D., Soulsby, C., & Laudon, H. (2015). Connecting precipitation inputs and soil flow pathways to stream water in contrasting boreal catchments. *Hydrological Processes*, *29*(16), 3546–3555. https://doi.org/10.1002/hyp.10300

Rothfuss, Y., & Javaux, M. (2017). Reviews and syntheses: Isotopic approaches to quantify root water uptake: a review and comparison of methods. *Biogeosciences*, *14*(8), 2199–2224. https://doi.org/10.5194/bg-14-2199-2017

Scheliga, B., Tetzlaff, D., Nuetzmann, G., & Soulsby, C. (2017). Groundwater isoscapes in a montane headwater catchment show dominance of well-mixed storage. *Hydrological Processes*, *31*(20), 3504–3519. https://doi.org/10.1002/hyp.11271

Serreze, M. C., & Barry, R. G. (2011). Processes and impacts of Arctic amplification: A research synthesis. *Global and Planetary Change*, *77*(1-2), 85–96. https://doi.org/10.1016/j.gloplacha.2011.03.004

Simonin, K. A., Link, P., Rempe, D., Miller, S., Oshun, J., Bode, C., Dietrich, W. E., Fung, I., & Dawson, T. E. (2014). Vegetation induced changes in the stable isotope composition of near surface humidity. *Ecohydrology*, *7*(3), 936–949. https://doi.org/10.1002/eco.1420

Smith, P., House, J. I., Bustamante, M., Sobocká, J., Harper, R., Pan, G., West, P. C., Clark, J. M., Adhya, T.,. . . Pugh, T. A. M. (2016). Global change pressures on soils from land use and management. *Global change biology*, *22*(3), 1008–1028. https://doi.org/10.1111/gcb.13068

Soulsby, C., Birkel, C., Geris, J., Dick, J., Tunaley, C., & Tetzlaff, D. (2015). Stream water age distributions controlled by storage dynamics and nonlinear hydrologic connectivity: Modeling with high-resolution isotope data. *Water Resources Research*, *51*(9), 7759–7776. https://doi.org/10.1002/2015WR017888

Soulsby, C., Braun, H., Sprenger, M., Weiler, M., & Tetzlaff, D. (2017). Influence of forest and shrub canopies on precipitation partitioning and isotopic signatures. *Hydrological Processes*, *31*(24), 4282–4296. https://doi.org/10.1002/hyp.11351

Sprenger, M., Seeger, S., Blume, T., & Weiler, M. (2016). Travel times in the vadose zone: variability in space and time. *Water Resources Research*, *52*(8), 5727–5754. https://doi.org/10.1002/2015WR018077

Sprenger, M., Erhardt, M., Riedel, M., & Weiler, M. (2016). Historical tracking of nitrate in contrasting vineyards using water isotopes and nitrate depth profiles. *Agric Ecosyst Environ (Agriculture, Ecosystems & Environment)*, *222*, 185–192. https://doi.org/10.1016/j.agee.2016.02.014

Sprenger, M., Herbstritt, B., & Weiler, M. (2015). Established methods and new opportunities for pore water stable isotope analysis. *Hydrological Processes*, *29*(25), 5174–5192. https://doi.org/10.1002/hyp.10643

Sprenger, M., Leistert, H., Gimbel, K., & Weiler, M. (2016). Illuminating hydrological processes at the soil-vegetation-atmosphere interface with water stable isotopes. *Reviews of Geophysics*, *54*(3), 674–704. https://doi.org/10.1002/2015RG000515

Sprenger, M., Tetzlaff, D., Buttle, J. M., Laudon, H., Leistert, H., Mitchell, C. P. J., Snelgrove, J., Weiler, M., & Soulsby, C. (2018). Measuring and modelling stable isotopes of mobile and bulk soil water. *Vadose Zone Journal.* Advance online publication. https://doi.org/10.2136/VZJ2017.08.0149

Sprenger, M., Tetzlaff, D., Buttle, J., Laudon, H., & Soulsby, C. (2018). Water ages in the critical zone of long-term experimental sites in northern latitudes. *Hydrol. Earth Syst. Sci. Discuss.*, 1–26. https://doi.org/10.5194/hess-2018-144

Sprenger, M., Tetzlaff, D., & Soulsby, C. (2017a). Soil water stable isotopes reveal evaporation dynamics at the soil-plant-atmosphere interface of the critical zone. *Hydrology and Earth System Sciences*, *21*(7), 3839–3858. https://doi.org/10.5194/hess-21-3839-2017

Sprenger, M., Tetzlaff, D., & Soulsby, C. (2017b). No influence of CO2 on stable isotope analyses of soil waters with OA-ICOS. *Rapid Communications in Mass Spectrometry*, *31*(5), 430–436. https://doi.org/10.1002/rcm.7815

Sprenger, M., Tetzlaff, D., Tunaley, C., Dick, J., & Soulsby, C. (2017). Evaporation fractionation in a peatland drainage network affects stream water isotope composition. *Water Resources Research*, *53*(1), 851–866. https://doi.org/10.1002/2016WR019258

Tappa, D. J., Kohn, M. J., McNamara, J. P., Benner, S. G., & Flores, A. N. (2016). Isotopic composition of precipitation in a topographically steep, seasonally snow-dominated watershed and implications of variations from the Global Meteoric Water Line. *Hydrological Processes*, *30*(24), 4582–4592. https://doi.org/10.1002/hyp.10940

Tesfa, T. K., Tarboton, D. G., Chandler, D. G., & McNamara, J. P. (2010). A Generalized Additive Soil Depth Model for a Mountainous Semi-Arid Watershed Based Upon Topographic and Land Cover Attributes. In J. L. Boettinger, D. W. Howell, A. C. Moore, A. E. Hartemink, & S. Kienast-Brown (Eds.), *Digital Soil Mapping: Bridging Research, Environmental Application, and Operation* (pp. 29–41). Dordrecht: Springer Netherlands. https://doi.org/10.1007/978-90-481-8863-5_3

Tetzlaff, D., Birkel, C., Dick, J., Geris, J., & Soulsby, C. (2014). Storage dynamics in hydropedological units control hillslope connectivity, runoff generation and the evolution of catchment transit time distributions. *Water Resources Research*, *50*(2), 969–985. https://doi.org/10.1002/2013WR014147

Tetzlaff, D., Buttle, J., Carey, S. K., McGuire, K., Laudon, H., & Soulsby, C. (2015). Tracer-based assessment of flow paths, storage and runoff generation in northern catchments: a review. *Hydrological Processes*, *29*(16), 3475–3490. https://doi.org/10.1002/hyp.10412

Tetzlaff, D., Buttle, J., Carey, S. K., van Huijgevoort, M. H. J., Laudon, H., McNamara, J., Mitchell, C. P. J., Spence, C., Gabor, R. S., & Soulsby, C. (2015). A preliminary assessment of water partitioning and ecohydrological coupling in northern headwaters using stable isotopes and conceptual runoff models. *Hydrological Processes*, *29*(25), 5153–5173. https://doi.org/10.1002/hyp.10515

Tetzlaff, D., Carey, S., Soulsby, C., Tetzlaff, D., Soulsby, C., Buttle, J., Capell, R., Carey, S. K., Laudon, H.,. . . Shanley, J. (2013). Catchments on the cusp? Structural and functional change in northern ecohydrology. *Hydrological Processes*, *27*(5), 766–774. https://doi.org/10.1002/hyp.9700

Timbe, E., Windhorst, D., Crespo, P., Frede, H.-G., Feyen, J., & Breuer, L. (2014). Understanding uncertainties when inferring mean transit times of water trough tracer-based lumped-parameter models in Andean tropical montane cloud forest catchments. *Hydrology and Earth System Sciences*, *18*(4), 1503–1523. https://doi.org/10.5194/hess-18-1503-2014

van der Velde, Y., Heidbüchel, I., Lyon, S. W., Nyberg, L., Rodhe, A., Bishop, K., & Troch, P. A. (2015). Consequences of mixing assumptions for time-variable travel time distributions. *Hydrological Processes*, *29*(16), 3460–3474. https://doi.org/10.1002/hyp.10372

van Huijgevoort, M. H. J., Tetzlaff, D., Sutanudjaja, E. H., & Soulsby, C. (2016). Using high resolution tracer data to constrain water storage, flux and age estimates in a spatially distributed rainfall-runoff model. *Hydrological Processes*, *30*(25), 4761–4778. https://doi.org/10.1002/hyp.10902

Wassenaar, L.I., Hendry, M.J., Chostner, V.L., & Lis, G.P. (2008). High Resolution Pore Water δ^2H and $\delta^{18}O$ Measurements by H 2 O (liquid) −H 2 O (vapor) Equilibration Laser Spectroscopy. *Environmental Science & Technology*, *42*(24), 9262–9267. https://doi.org/10.1021/es802065s

West, A. G., Patrickson, S. J., & Ehleringer, J. R. (2006). Water extraction times for plant and soil materials used in stable isotope analysis. *Rapid Communications in Mass Spectrometry*, *20*(8), 1317–1321. https://doi.org/10.1002/rcm.2456

Windhorst, D., Kraft, P., Timbe, E., Frede, H.-G., & Breuer, L. (2014). Stable water isotope tracing through hydrological models for disentangling runoff generation processes at the hillslope scale. *Hydrology and Earth System Sciences*, *18*(10), 4113–4127. https://doi.org/10.5194/hess-18-4113-2014

Xu, L., Myneni, R. B., Chapin III, F. S., Callaghan, T. V., Pinzon, J. E., Tucker, C. J., Zhu, Z., Bi, J., Ciais, P.,. . . Stroeve, J. C. (2013). Temperature and vegetation seasonality diminishment over northern lands. *Nature Climate Change*, *3*, 581–586. https://doi.org/10.1038/nclimate1836

Zapata-Rios, X., McIntosh, J., Rademacher, L., Troch, P. A., Brooks, P. D., Rasmussen, C., & Chorover, J. (2015). Climatic and landscape controls on water transit times and silicate mineral weathering in the critical zone. *Water Resources Research*, *51*(8), 6036–6051. https://doi.org/10.1002/2015WR017018

Zeng, X. (2001). Global Vegetation Root Distribution for Land Modeling. *Journal of Hydrometeorology*, *2*(5), 525–530. https://doi.org/10.1175/1525-7541(2001)002<0525:GVRDFL>2.0.CO;2

Zhang, W., An, S., Xu, Z., Cui, J., & Xu, Q. (2011). The impact of vegetation and soil on runoff regulation in headwater streams on the east Qinghai–Tibet Plateau, China. *CATENA*, *87*(2), 182–189. https://doi.org/10.1016/j.catena.2011.05.020

Table 1: Environmental characteristics of each study site: Average values of precipitation sum (P), air temperature (T), potential evapotranspiration (PET), and number of dry days for 12 months during the sampling period (Table 2); soil type, soil texture description, vegetation cover, elevation and groundwater depth at the sampling locations within the five long-term experimental catchments. OM = organic matter content.

Catchment	Location	P [mm year^{-1}]	T [°C]	PET [mm year^{-1}]	Dry days year^{-1}	Soil texture	Vegetation cover	Elevation [m a.s.l.]	Groundwater depth [m]
Dry Creek	LG	496	9.5±9.1	695	246	Loam to sandy loam	Ponderosa pine (*Pinus ponderosa*) and Douglas-fir (*Pseudotsuga menziesii*)	1150	> 2
	TL	787	8.1±9.5	671	245		Willow dominated	1610	> 2
Bruntland Burn	NF	1332	7.2±4.7	488	116	Loamy sand, OM = 5-20%	Scots pine (*Pinus sylvestris*)	260	> 0.5
	NH						Erica species (*Calluna vulgaris*)	260	> 0.5
	SF						Scots pine (*Pinus sylvestris*)	270	> 1
	SH						Erica species (*Calluna vulgaris*)	270	> 1
Dorset	Or	1125	6.7±11.1	898	249	Sandy loam, OM = 4%	Red oak (*Quercus rubra*)	365	> 0.5
	He						Eastern hemlock (*Tsuga canadensis*)	370	> 0.5
	Ce						Eastern white cedar (*Thuja occidentalis*)	365	> 0.5
	Pw						White pine (*Pinus strobus*)	365	> 0.5
Krycklan	S04	687	3.2±8.7	462	249	Sand, OM = 80 %	Norway spruce (*Picea abies*)	267	> 0.3
	S22					Sand, OM = 5%	Scots pine (*Pinus sylvestris*)	270	> 0.5
Wolf Creek	PL	440	0.28±8.4	432	280	Silty sand, OM = 7 %	Birch (*Betulaceae nana*)	1440	0.6 - 2
	RP					Silty sand, OM = 70 %	Willow (*Salix spec.)*	1370	0.1 – 0.3

Table 2: Isotope sampling design (number of sampling campaigns, sampling period, maximum sampling depth, and total sample number), mean volumetric soil moisture at 10 cm (VSM) and isotopic characteristics of the precipitation (P) and soil waters in the upper 30 cm.

Site	Location	Sampling campaigns	Sampling period	Max. sampling depth [cm]	Total sample number	VSM [cm^3 cm^{-3}]	P δ^2H [‰]	Soil water δ^2H [‰]	Soil water lc-excess [‰]
Dry Creek	LG	9	2011-06-29 – 2012-09-13	-70	119	0.25±0.08	-105.2±25.0	-118.1±12.4	-18.1±18.0
	TL	7	2011-08-11 – 2012-09-07		132	0.15±0.07	-113.8±25.7	-125±14.1	-8.5±17.7
Bruntland Burn	NF	11	2015-09-29 – 2016-09-23	-20	215	0.46±0.05	-52.8±25.0	-52.0±11.1	-3.6±4.9
	NH	11			218	0.33±0.03		-51.1±10.8	-2.0±3.6
	SF	11			214	0.46±0.05		-50.5±10.2	-3.7±4.5
	SH	11			211	0.33±0.03		-53.1±8.9	-2.7±3.6
Dorset	Or	6	2015-10-26 – 2016-11-04	-50	193	0.28±0.09	-76.7±26.3	-52.2±12.1	-2.0±6.5
	He	6			187			-55.1±9.9	-3.7±6.7
	Ce	6			151			-54.8±11.0	-4.2±5.1
	Pw	6			182			-51.5±10.8	-4.5±6.7
Krycklan	S04	7	2015-09-22 – 2016-09-20	-30	164	0.72±0.07	-102.8±32.5	-88.2±5.0	0.4±2.2
	S22	7			149	0.19±0.04		-80.5±8.4	0.2±2.7
Wolf Creek	PL	9	2015-08-25 – 2016-09-20	-85	49	0.12±0.12	-143.8	-154.6±11.1	-5.4±15.7
	RP	10	2015-06-27 – 2016-09-19	-40	52	0.42±0.11		-159.8±8.8	-8.3±14.1

Table 3 Results of multiple linear regression models to explain the soil water lc-excess data pooled for each sampling site over different time periods: all available data, spring, summer, and autumn (as shown in Figure 6). The significance level for each parameter is given according to ANOVA of the linear models. *** = p<0.001; **=p<0.01; *=p<0.05, •=p<0.10, n.s. indicates parameters that were not significant for the model. Percentage in brackets show the relative importance of the explanatory parameter. Note that the lc-excess data was reciprocally transformed for "All data" and "Summer" to get normal distributions and that the lc-excess of the samples taken in autumn was not normally distributed.

Multiple linear model	All data	Spring	Summer	Autumn
Multiple r^2 (adjusted)	0.88 (0.87)	0.74 (0.70)	0.87 (0.84)	0.98 (0.97)
Factors			Estimate	
Intercept	-0.75±0.238	1.89±0.53	-0.43±0.18	9.84±0.79
P_{30}			0.31±0.04*** (83 %)	-0.01±0.16*** (27 %)
P_7	0.23 (100 %)	0.80±0.15 (81 %)		
T_{30}		0.42±0.15* (19 %)	0.12±0.04* (17 %)	-3.22±0.23*** (26 %)
VSM	n.s.	n.s.	n.s.	-3.36±0.26** (9 %)
P_{30}:T_{30}		n.s.	n.s.	-0.21±0.07** (3 %)
T_{30}:VSM	n.s.	n.s.	n.s.	2.23±0.16*** (35 %)

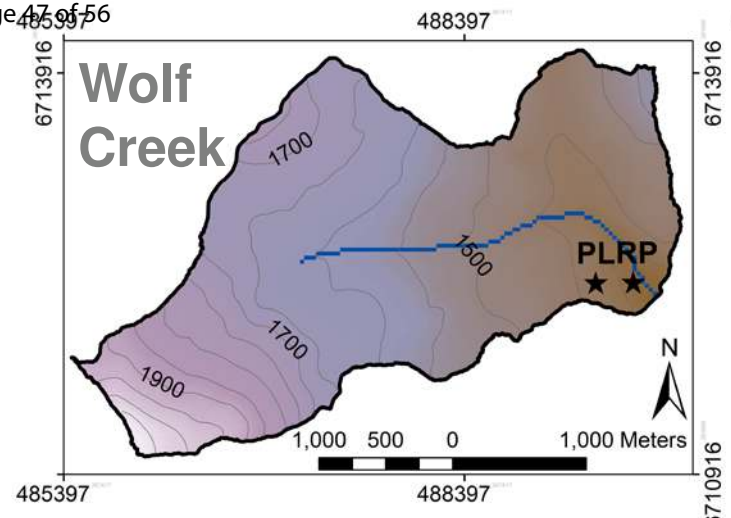
Wolf Creek
485397
488397
6713916
6710916
1700
1600
1900
PLRP
N
1,000 500 0 1,000 Meters

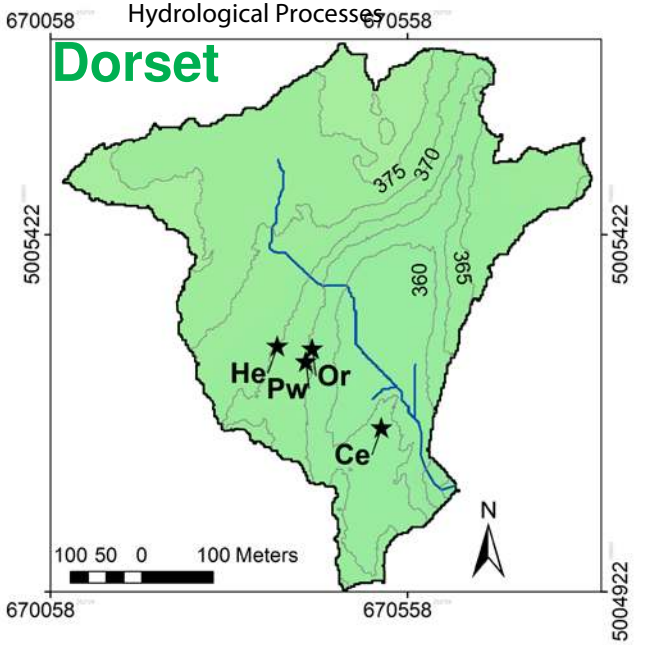
Dorset
670058
670558
5005422
5004922
375
370
360
365
He
Pw
Or
Ce
N
100 50 0 100 Meters

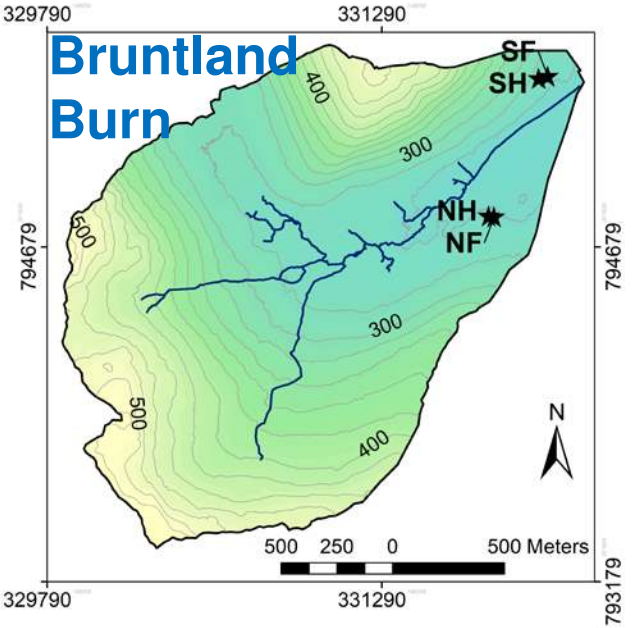
Bruntland Burn
329790
331290
794679
793179
SF
SH
NH
NF
400
300
600
500
N
500 250 0 500 Meters

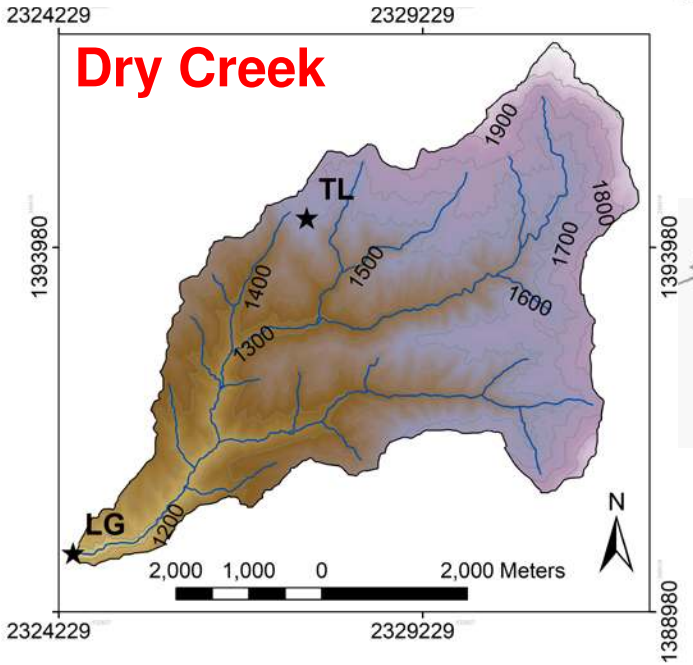
Dry Creek
2324229
2329229
1393980
1388980
TL
LG
1900
1800
1700
1600
1500
1400
1300
1200
N
2,000 1,000 0 2,000 Meters

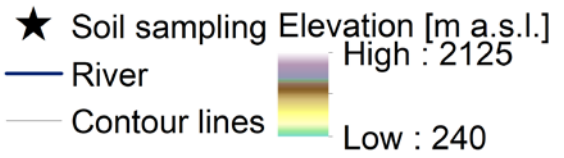
Soil sampling Elevation [m a.s.l.]
River
Contour lines
High : 2125
Low : 240

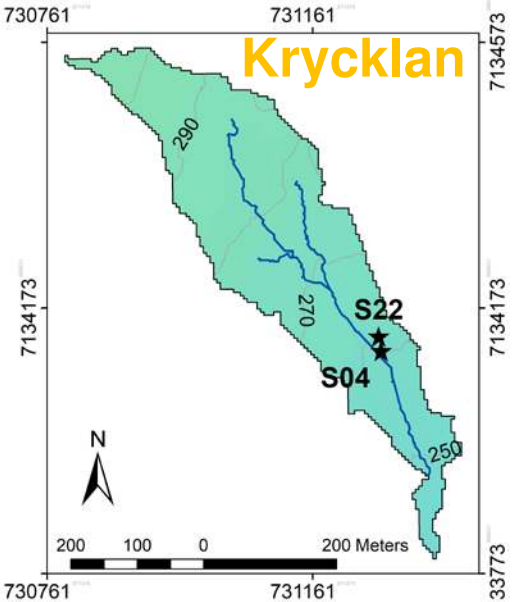
Krycklan
730761
731161
7134573
7134173
7133773
290
270
250
S22
S04
N
200 100 0 200 Meters

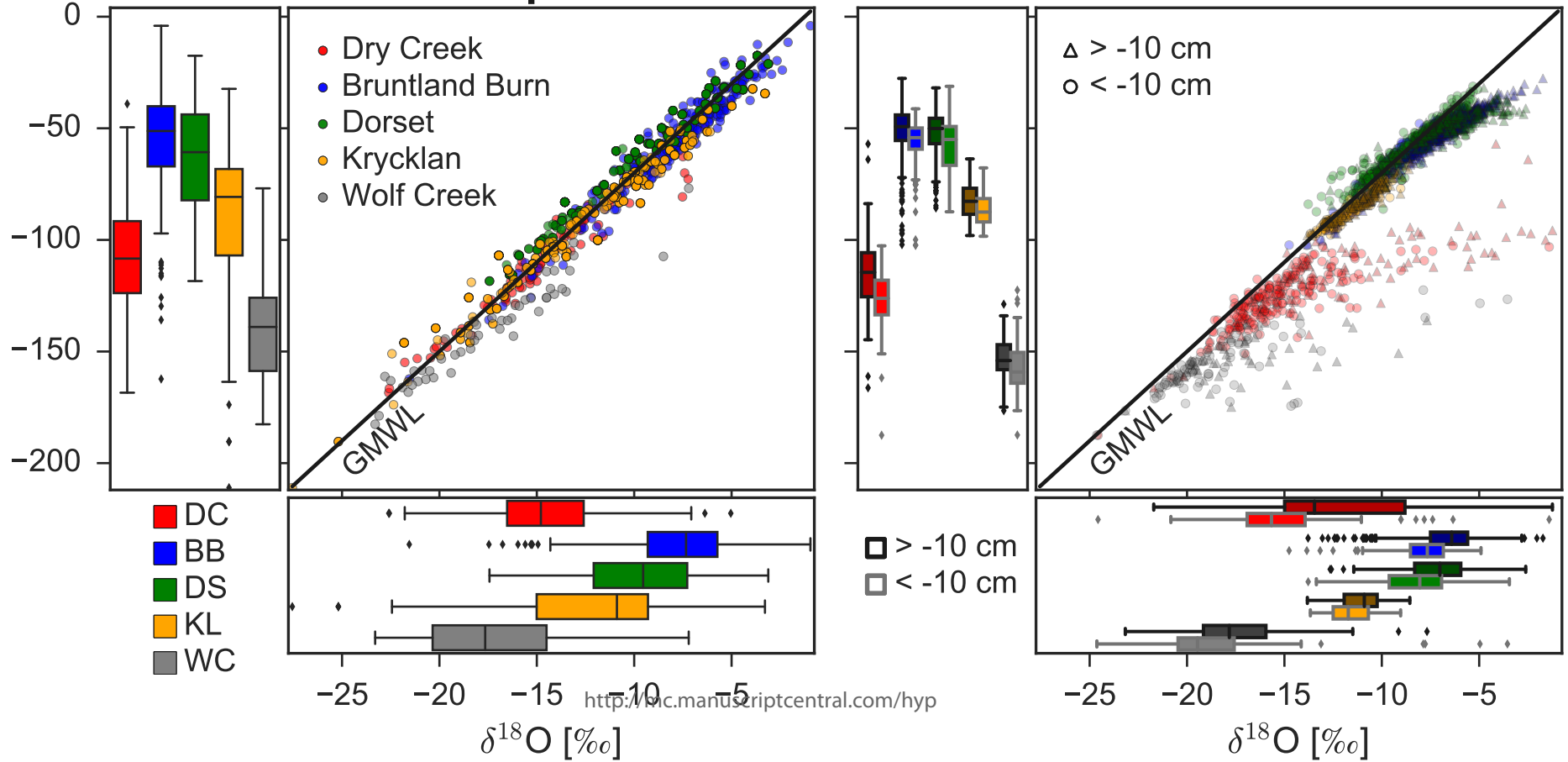

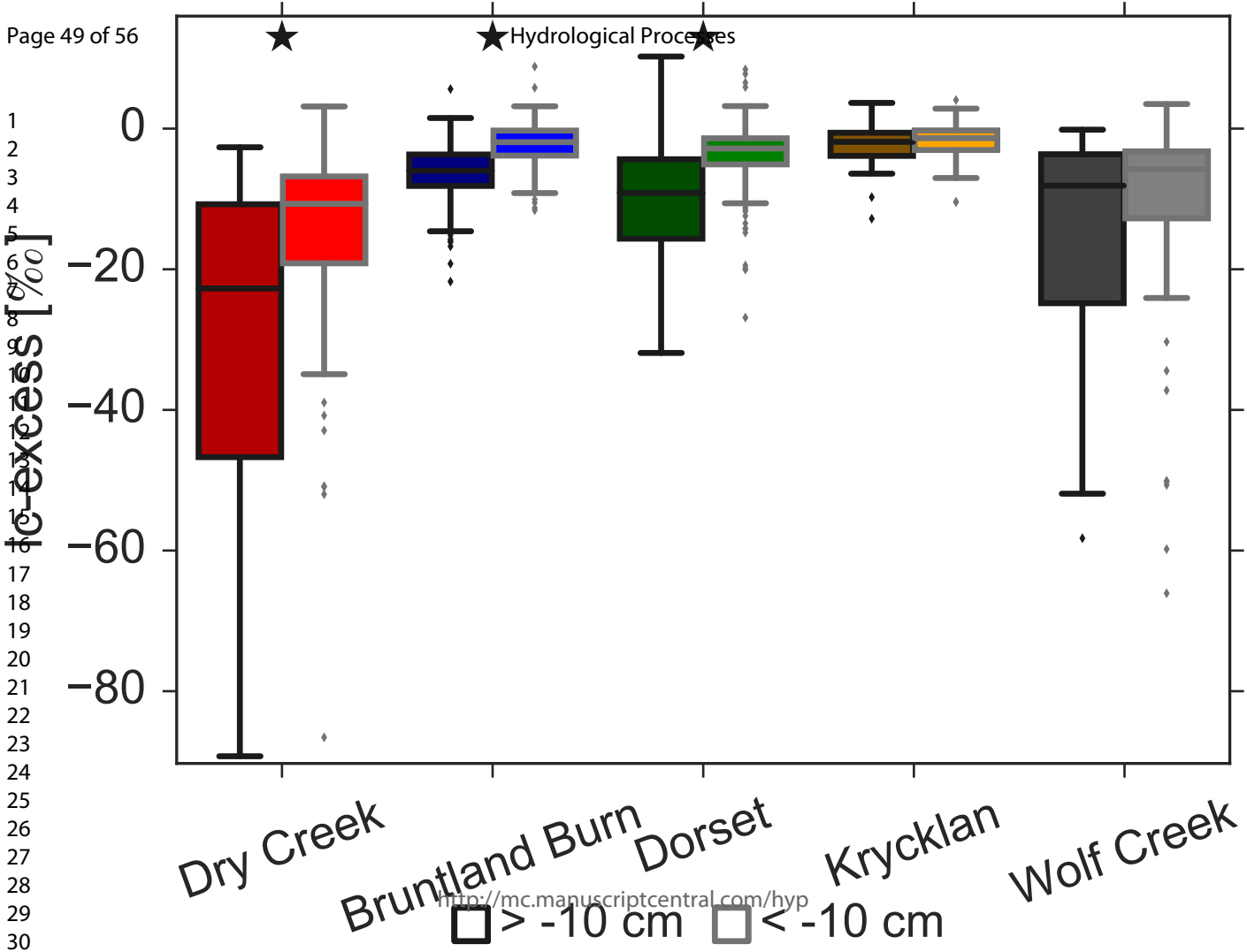

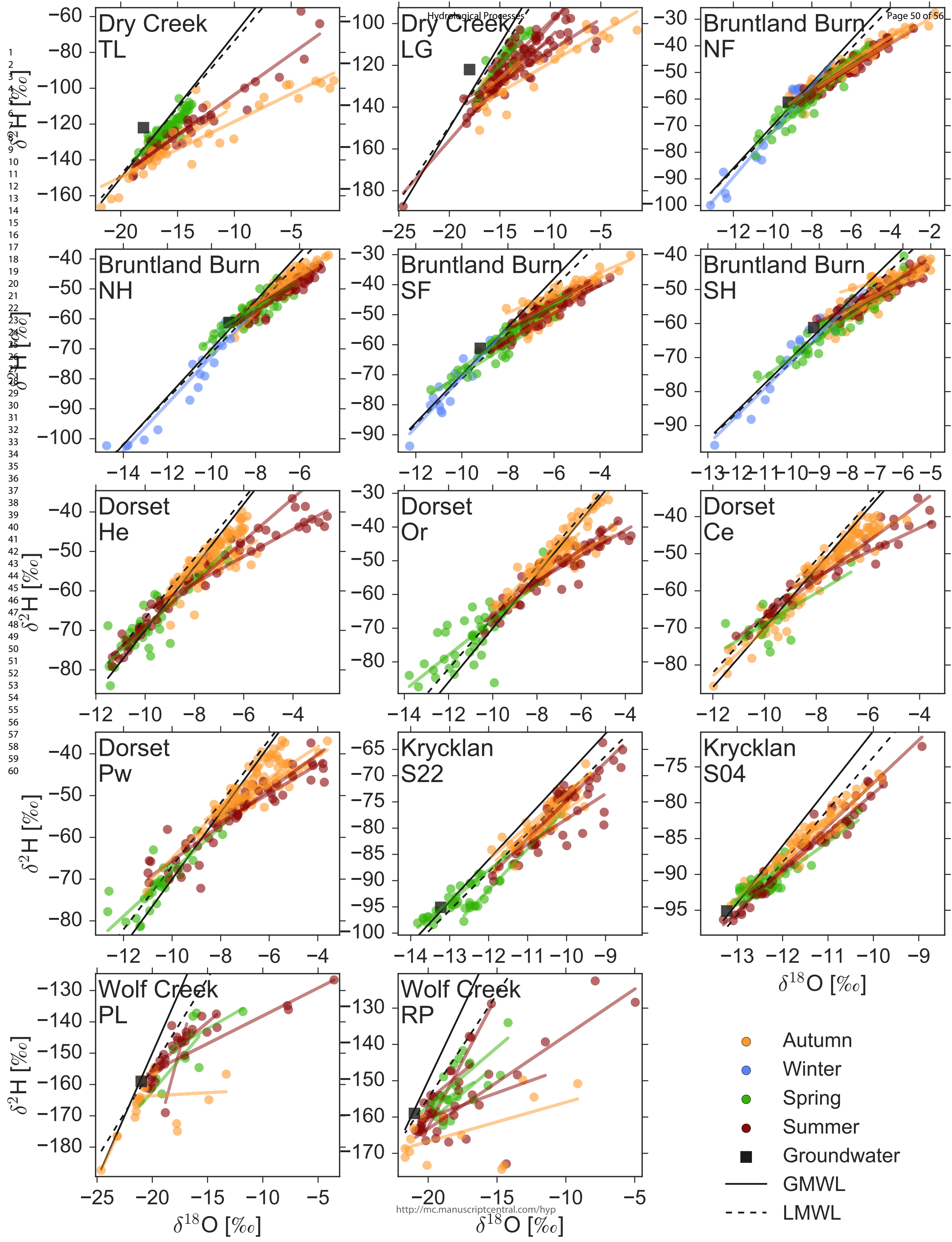
Dry Creek
TL
Dry Creek
LG
Bruntland Burn
NF
Bruntland Burn
NH
Bruntland Burn
SF
Bruntland Burn
SH
Dorset
He
Dorset
Or
Dorset
Ce
Dorset
Pw
Krycklan
S22
Krycklan
S04
Wolf Creek
PL
Wolf Creek
RP
δ^2H [‰]
δ^{18}O [‰]
Autumn
Winter
Spring
Summer
Groundwater
GMWL
LMWL

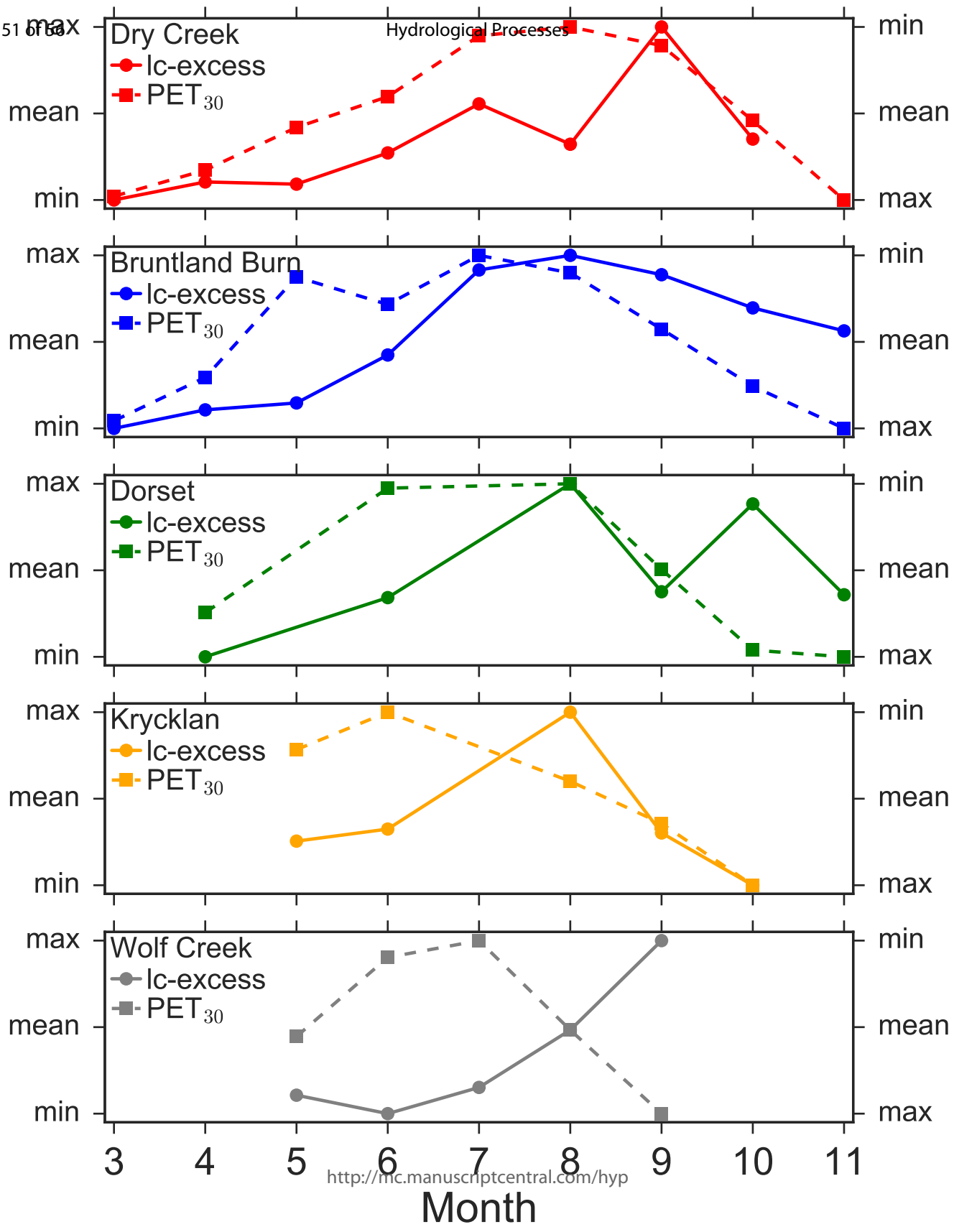
Dry Creek
lc-excess
PET30
Bruntland Burn
lc-excess
PET30
Dorset
lc-excess
PET30
Krycklan
lc-excess
PET30
Wolf Creek
lc-excess
PET30
max
mean
min
Unity-based normalization of PET30
Unity-based normalization of lc-excess
3
4
5
6
7
8
9
10
11
Month

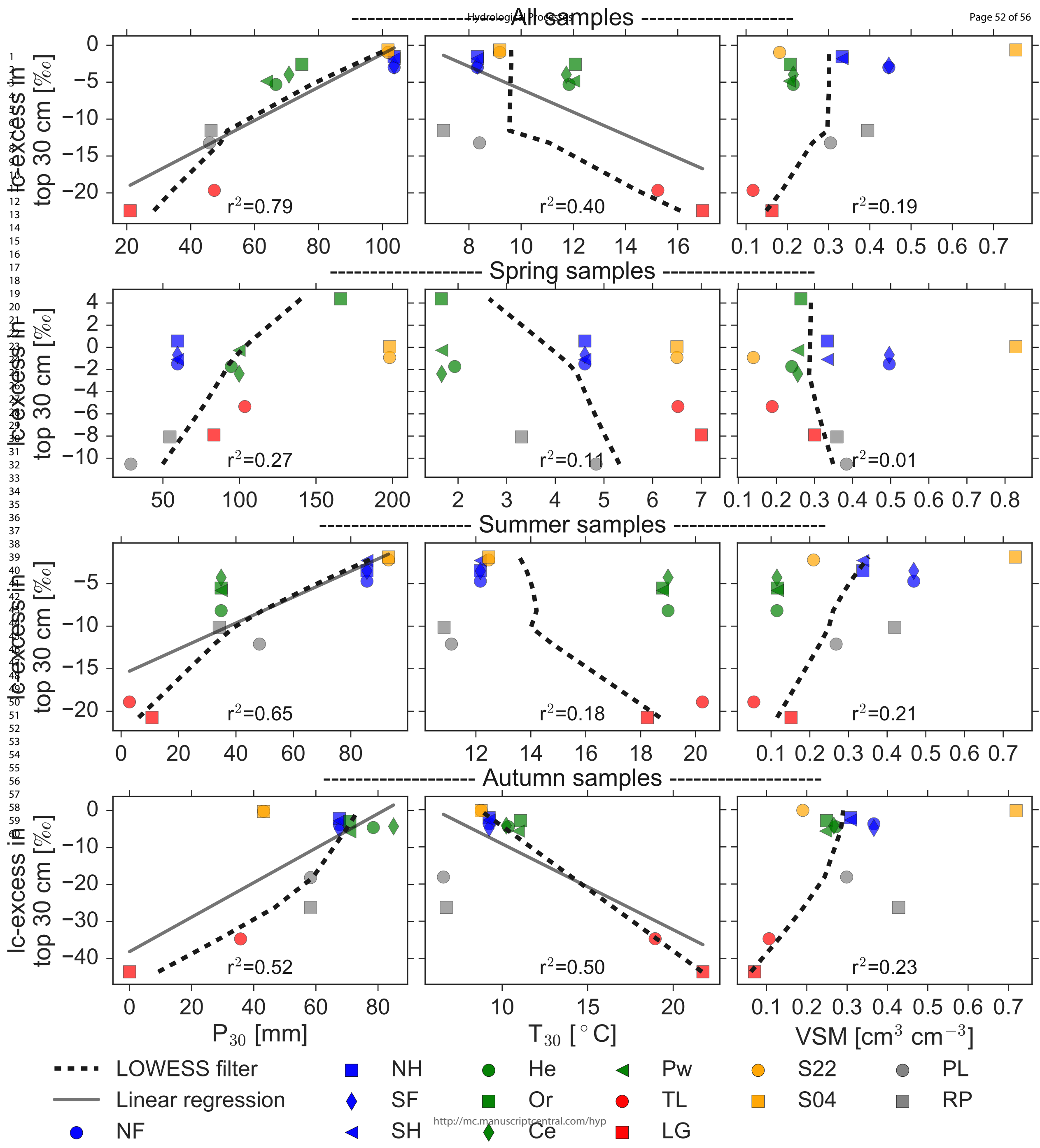

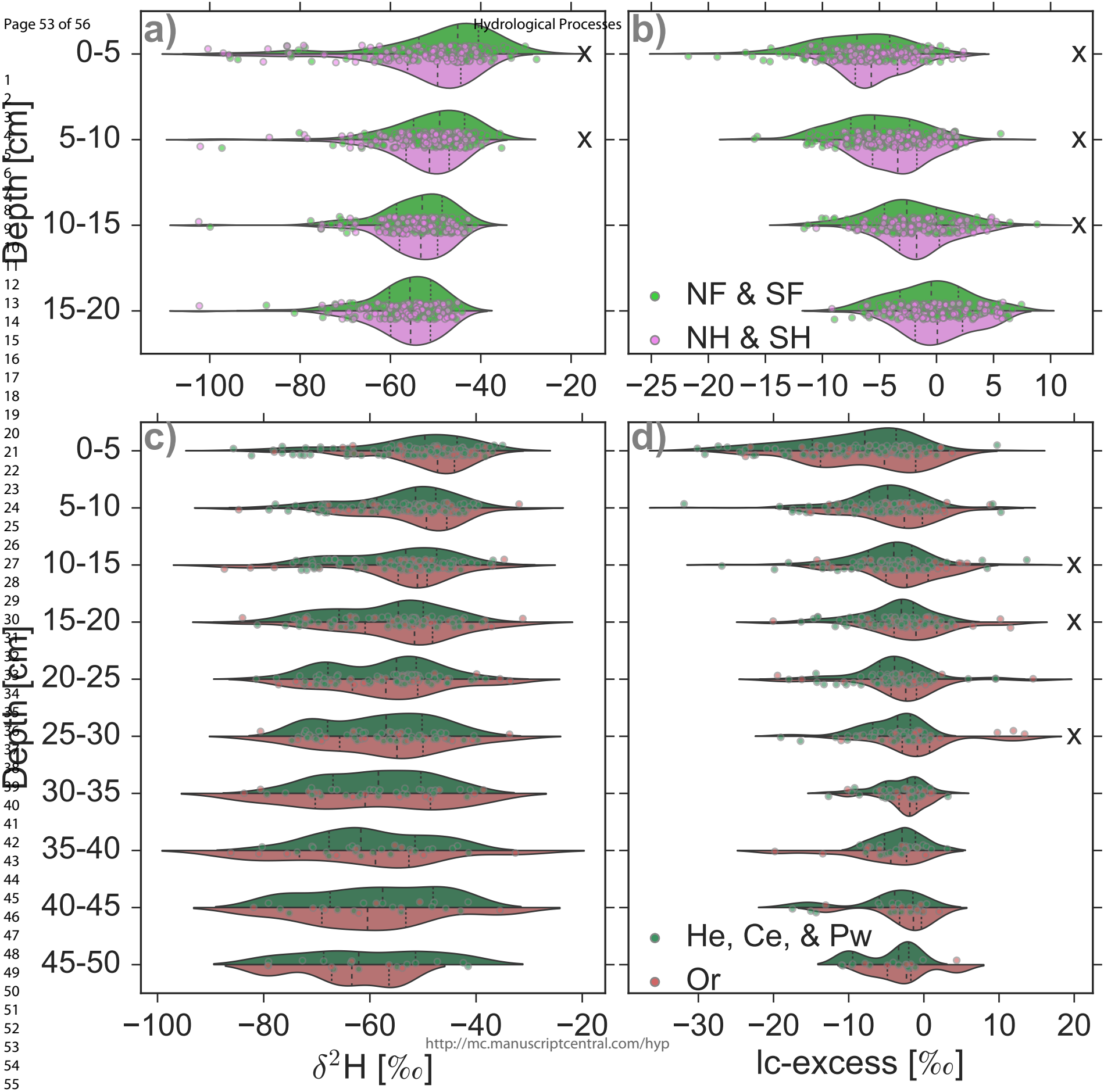
a)
b)
c)
d)
0-5
5-10
10-15
15-20
20-25
25-30
30-35
35-40
40-45
45-50
Depth [cm]
NF & SF
NH & SH
He, Ce, & Pw
Or
−100 −80 −60 −40 −20
−25 −20 −15 −10 −5 0 5 10
−30 −20 −10 0 10 20
δ²H [‰]
lc-excess [‰]

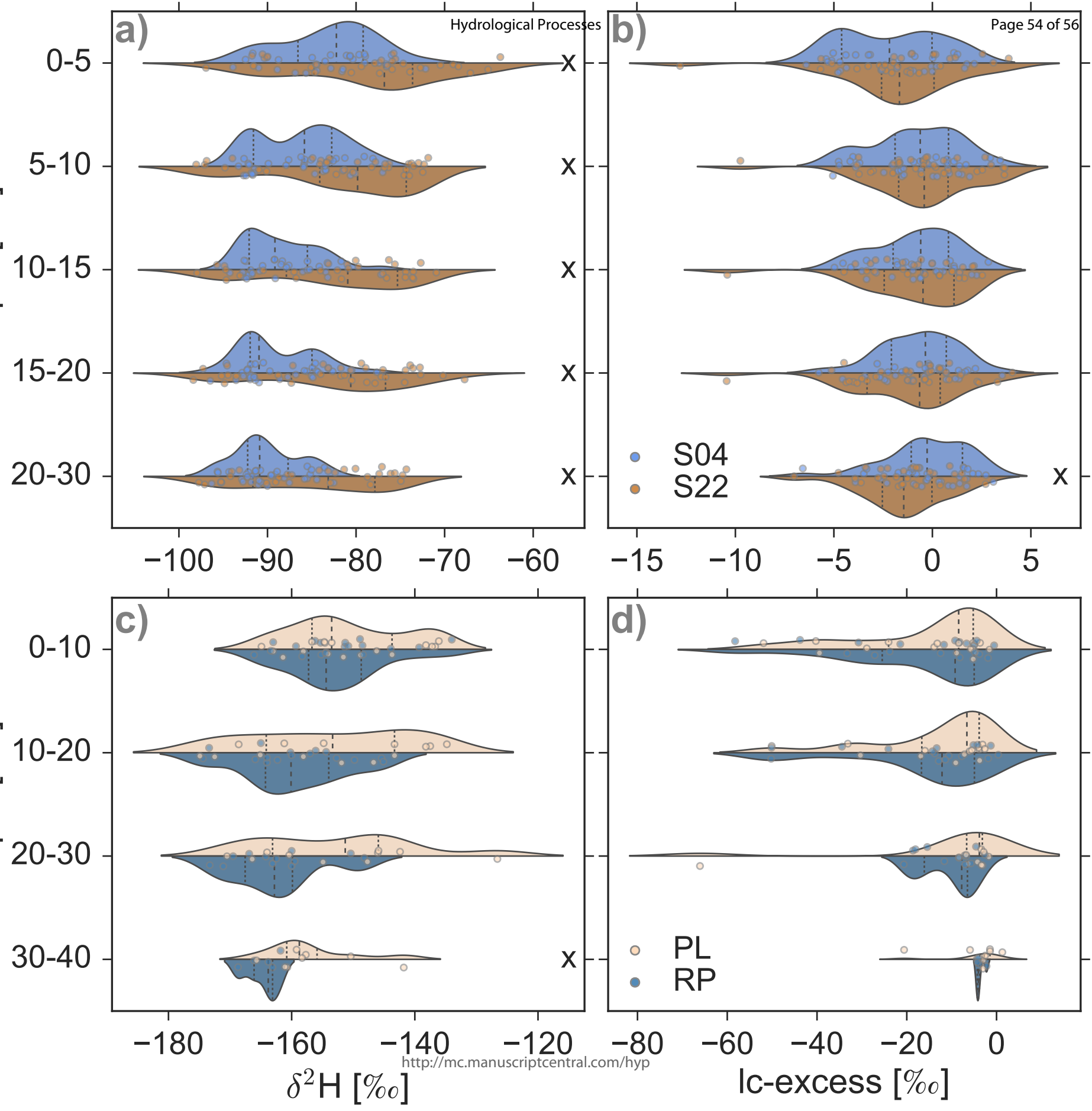
a)
b)
c)
d)
0-5
5-10
10-15
15-20
20-30
0-10
10-20
20-30
30-40
Depth [cm]
S04
S22
PL
RP
−100 −90 −80 −70 −60
−15 −10 −5 0 5
−180 −160 −140 −120
−80 −60 −40 −20 0
δ²H [‰]
lc-excess [‰]

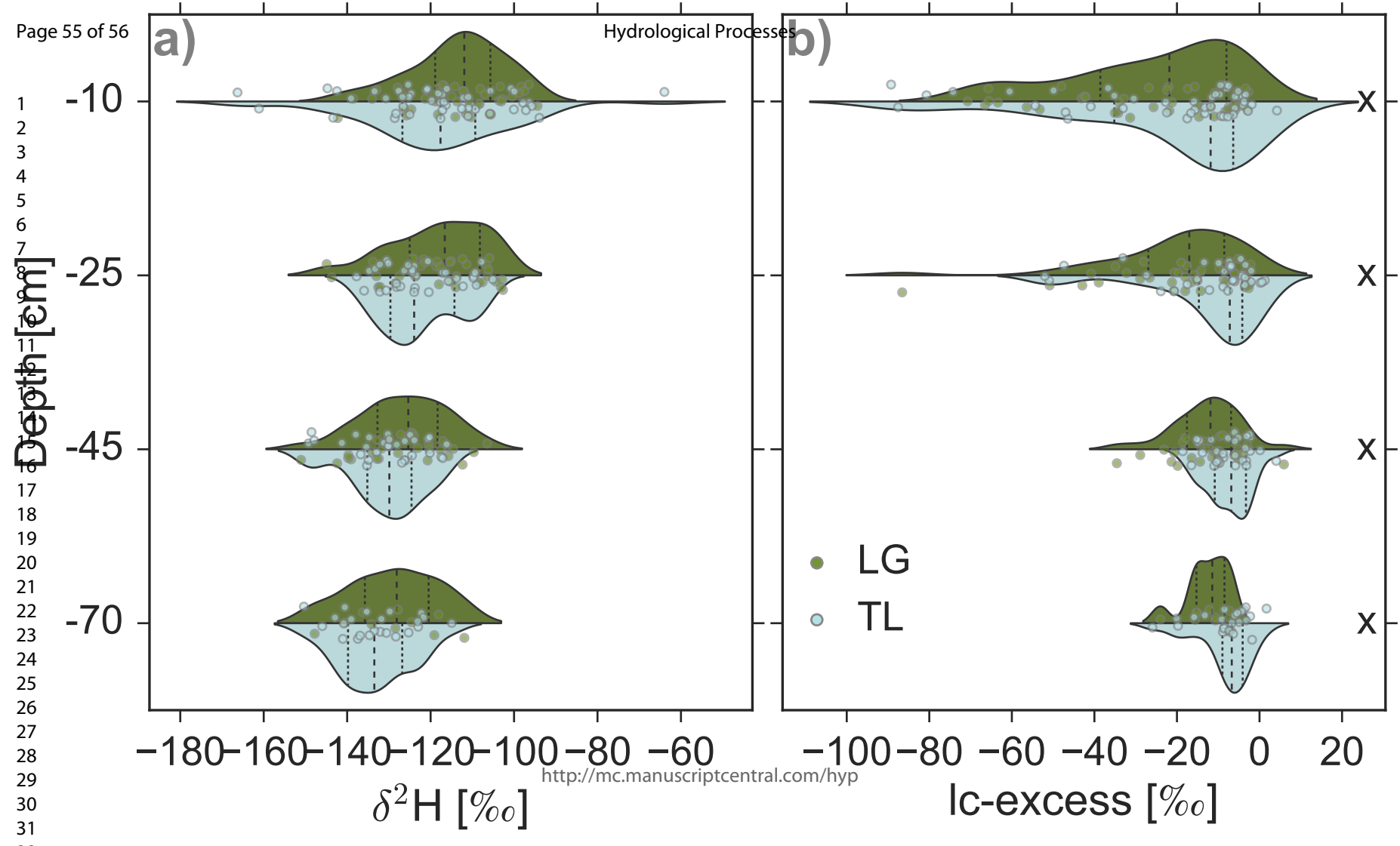
a)
b)
-10
-25
-45
-70
Depth [cm]
LG
TL
−180 −160 −140 −120 −100 −80 −60
δ^2H [‰]
−100 −80 −60 −40 −20 0 20
lc-excess [‰]

Soil depth	r P_2	r P_7	r P_{14}	r P_{30}	m P_{30}	Site	
-10	0.54	0.69	0.30	0.00	0.00	TL	Dry Creek
-25	-0.05	0.00	-0.29	-0.74	-0.15		
-45	-0.05	0.06	-0.33	-0.77	-0.15		
-10	-0.23	-0.23	-0.16	-0.37	-0.07	LG	
-25	-0.23	-0.23	-0.17	-0.37	-0.07		
-45	0.09	0.09	0.01	0.09	0.04		
-2.5	0.23	**0.59**	**0.89**	**0.77**	**1.00**	NF	Brutnland Burn
-7.5	0.18	0.41	**0.78**	**0.87**	**0.66**		
-12.5	0.18	0.30	**0.68**	**0.86**	**0.61**		
-17.5	0.13	0.19	0.47	**0.79**	**0.53**		
-2.5	0.25	0.58	**0.89**	**0.71**	**0.92**	NH	
-7.5	0.21	0.43	**0.78**	**0.64**	**0.60**		
-12.5	0.25	0.37	**0.73**	**0.67**	**0.50**		
-17.5	0.30	0.39	**0.72**	**0.78**	**0.64**		
-2.5	0.28	**0.62**	**0.91**	**0.78**	**0.99**	SF	
-7.5	0.24	0.52	**0.80**	**0.87**	**0.73**		
-12.5	0.39	0.48	**0.69**	**0.87**	**0.66**		
-17.5	0.46	0.46	**0.74**	**0.92**	**0.69**		
-2.5	0.16	0.56	**0.89**	**0.74**	**0.87**	SH	
-7.5	0.09	0.37	**0.76**	**0.85**	**0.63**		
-12.5	0.05	0.11	0.42	**0.76**	**0.48**		
-17.5	0.14	0.20	0.47	**0.78**	**0.50**		
-2.5	**0.88**	**0.80**	0.38	**0.97**	**0.64**	S22	Krycklan
-7.5	0.67	**0.77**	0.35	**0.96**	**0.59**		
-12.5	0.75	**0.80**	0.15	**0.92**	**0.59**		
-17.5	0.48	0.72	0.01	**0.83**	**0.56**		
-25.0	0.63	**0.86**	0.16	**0.81**	**0.46**		
-2.5	0.78	**0.96**	0.43	**0.92**	**0.32**	S04	
-7.5	0.16	0.67	0.13	0.49	0.17		
-12.5	0.27	0.70	0.02	0.34	0.10		
-17.5	-0.02	0.45	-0.09	0.22	0.07		
-25.0	-0.22	0.29	-0.18	-0.01	0.00		

Color bar:	-1.00	0.00	0.50	1.00

Soil depth	r P_2	r P_7	r P_{14}	r P_{30}	m P_{30}	Site	
-2.5	0.67	**0.80**	0.77	**0.82**	**0.36**	He	Dorset
-7.5	0.31	0.26	0.25	0.64	0.23		
-12.5	0.07	0.27	0.33	0.49	0.19		
-17.5	-0.24	-0.21	-0.13	0.22	0.12		
-22.5	-0.29	-0.31	-0.24	0.16	0.08		
-27.5	-0.15	-0.20	-0.13	0.31	0.16		
-32.5	-0.17	-0.30	-0.24	0.27	0.14		
-2.5	0.41	**0.80**	0.77	0.46	0.26	Or	
-7.5	0.27	0.39	0.64	0.67	0.47		
-12.5	0.26	0.26	0.54	0.72	0.65		
-17.5	-0.01	0.17	0.54	0.65	0.56		
-22.5	0.03	-0.05	0.30	0.57	0.50		
-27.5	-0.04	-0.14	0.23	0.49	0.43		
-32.5	-0.15	-0.22	0.11	0.34	0.35		
-2.5	**0.85**	**0.96**	**0.89**	**0.89**	**0.67**	Ce	
-7.5	0.70	0.79	0.74	**0.90**	**0.47**		
-12.5	0.32	0.41	0.41	0.69	0.39		
-17.5	0.28	0.32	0.34	0.70	0.40		
-22.5	0.24	0.17	0.22	0.68	0.34		
-27.5	0.13	0.06	0.11	0.57	0.35		
-32.5	-0.04	0.00	-0.06	0.30	0.17		
-2.5	0.02	0.65	**0.83**	0.68	0.34	Pw	
-7.5	-0.16	0.21	0.57	0.69	0.38		
-12.5	-0.22	-0.01	0.43	0.57	0.38		
-17.5	-0.35	-0.06	0.39	0.47	0.32		
-22.5	-0.27	0.02	0.41	0.58	0.44		
-27.5	-0.19	-0.11	0.28	0.58	0.44		
-32.5	-0.32	-0.25	0.40	0.44	0.36		
-5	0.41	0.39	0.52	0.71	0.28	PL	Wolf Creek
-15	0.00	0.06	0.56	0.59	0.43		
-25	0.63	0.72	0.74	0.70	0.40		
-35	0.07	0.26	0.34	0.06	0.02		
-5	-0.43	0.01	-0.19	0.15	0.03	RP	
-15	0.12	0.04	0.16	-0.01	-0.01		